minerals

MDPI

Review

Sulfates from the Pyrite Ore Deposits of the Apuan Alps (Tuscany, Italy): A Review

Cristian Biagioni, Daniela Mauro * and Marco Pasero

Dipartimento di Scienze della Terra, Università di Pisa, Via Santa Maria 53, I-56126 Pisa, Italy; cristian.biagioni@unipi.it (C.B.); marco.pasero@unipi.it (M.P.)

* Correspondence: daniela.mauro@dst.unipi.it; Tel.: +39-050-221-5789

Received: 9 November 2020; Accepted: 2 December 2020; Published: 5 December 2020

Abstract: The occurrence of sulfate minerals associated with the pyrite ores of the southern Apuan Alps has been known since the 19th century but modern mineralogical studies started only in the last decade. Sulfate assemblages were identified in all the pyrite ore deposits from the studied area but the more impressive associations were discovered in the Fornovolasco and Monte Arsiccio mines. Their study allowed to improve the knowledge of the sulfate crystal-chemistry and to achieve a better understanding of the acid mine drainage (AMD) systems associated with pyrite oxidation. More than 20 different mineral species were identified and, among them, four sulfates (volaschioite, giacovazzoite, magnanelliite, and scordariite) have their type localities in the pyrite ore deposits of the Apuan Alps. A review of the mineralogical results of a ten-year-long study is given here.

Keywords: sulfate minerals; pyrite oxidation; new mineral species; crystal-chemistry; Apuan Alps; Italy

1. Introduction

The occurrence of secondary sulfate assemblages associated with the pyrite ore bodies from the Apuan Alps (Tuscany, Italy) has been reported since the second half of the 19th century (e.g., [1]). However, few species were described and some of them were doubtful. For instance, D'Achiardi [1] reported the presence of gypsum, melanterite, halotrichite, alum-(K), goslarite, and, possibly, coquimbite. Since the second half of the 2000s, the mineralogical study of the pyrite ± baryte ± iron oxide ore deposits from the southern Apuan Alps led to the identification of some interesting sulfate assemblages in which rare or even new mineral species were identified. The sulfate assemblages from the Fornovolasco mine were the first to be systematically studied using modern analytical techniques, spurred by the identification of the new mineral species volaschioite, $Fe^{3+}{}_4(SO_4)O_2(OH)_6{\cdot}2H_2O$ [2]. Later, Mauro et al. [3] identified a new hydrated iron phosphate-sulfate from the Buca della Vena mine and named it bohuslavite, $Fe^{3+}{}_4(PO_4)_3(SO_4)(OH)(H_2O)_{10}{\cdot}nH_2O$. The most recent discovery is a sulfate assemblage found at the Monte Arsiccio mine, where well-crystallized sulfate specimens were discovered, including three new mineral species [4–6]. In this paper, the results of a ten-year-long study are reviewed and summarized, along with some still unpublished results.

2. Geological Background

The pyrite ± baryte ± iron oxide ore deposits of the southern portion of the Apuan Alps (northern Tuscany, Italy) are located along a NE–SW belt, 10 km in length, from the hamlet of Fornovolasco, in Garfagnana, to the Valdicastello Carducci village, in Versilia (Figure 1). Five main mining sites are known. From NE to SW they are the Fornovolasco, Buca della Vena, Canale della Radice, Monte Arsiccio, and Pollone mines. At these localities, the relative abundance of pyrite, baryte, and iron oxides (magnetite, hematite, "limonite") is widely variable. For instance, at Fornovolasco and

Canale della Radice, baryte occurs only as an accessory mineral, whereas it forms large ore bodies at the Monte Arsiccio and Pollone mines. Pyrite is widespread in all these localities, although its abundance, texture, and geochemistry are highly variable. George et al. [7] described the textural and trace element evolution of pyrite ores from these deposits, showing the occurrence of several potentially toxic heavy elements, confirming previous data reported by Biagioni et al. [8] and D'Orazio et al. [9].

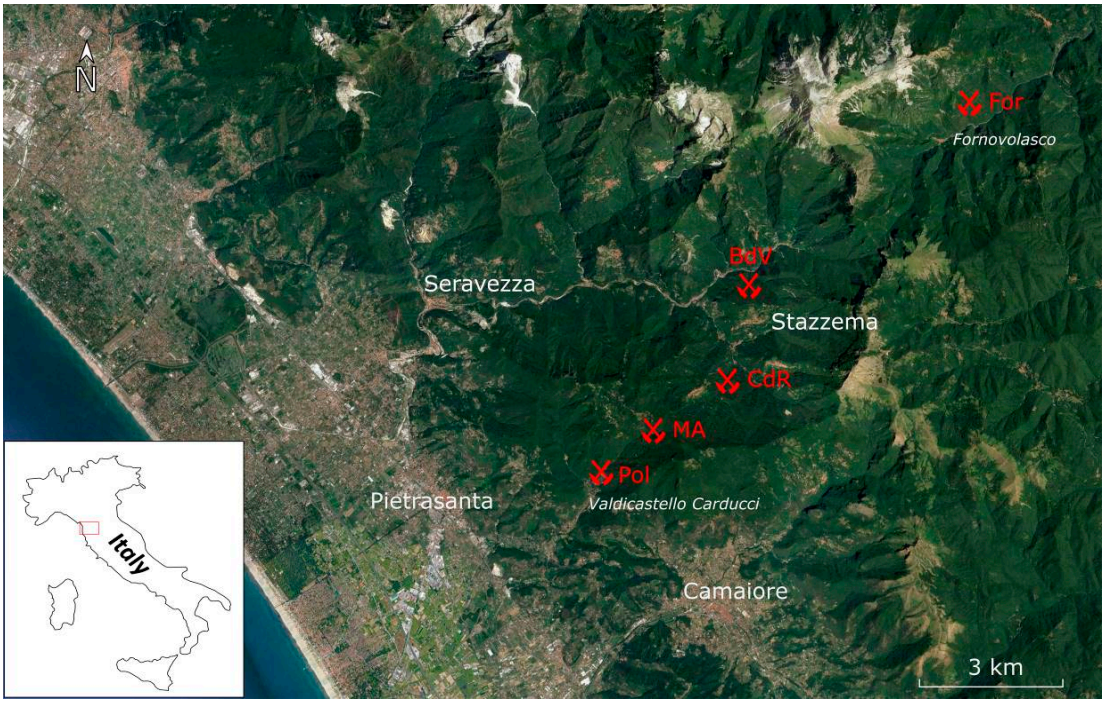

Figure 1. Map showing the localities cited in the text. Labels: BdV = Buca della Vena mine; CdR = Canale della Radice mine; For = Fornovolasco mine; MA = Monte Arsiccio mine; Pol = Pollone mine.

The main orebodies are hosted within the Apuane Unit and, in particular, in a Paleozoic metavolcanic-metasedimentary sequence, locally tourmalinized, and close to the contact with overlying Triassic metadolostone belonging to the "Grezzoni" Formation. A review of the main geological features of these deposits is given in [9,10].

The previous mining activity, along with the setting of the ore deposits, located close to the contact between a virtually impermeable phylladic basement and a strongly fractured and karstified carbonatic cover (metadolostone, marble), favoured the deep oxidation of some ore bodies, giving origin to some limonitic lenses that were, in some cases, exploited for iron production. The pervasive groundwater circulation, enhanced by high rainfall characterizing the Apuan Alps (more than 3000 mm/y [11]), is also responsible for the formation of some secondary sulfate assemblages, discovered only in the last decade. These assemblages may play a key role in determining the budget of heavy metals and acidity of acid mine drainage (AMD) systems occurring at some former mining sites in the Apuan Alps [12].

3. Secondary Sulfate Mineralogy from the Apuan Alps

Sulfate minerals occur in all the studied pyrite deposits (Table 1), although only some localities have been investigated in detail so far. Consequently, the large number of species reported from the Fornovolasco and Monte Arsiccio mines may be due to a sampling bias, owing to the finding of sulfate assemblages with well-crystallized phases; on the contrary, such phases may be absent or still undiscovered at the Buca della Vena, Canale della Radice, and Pollone mines.

Table 1. Secondary sulfate minerals from the pyrite ore deposits of the southern Apuan Alps.

Mineral	BdV	CdR	For	MA	Pol
Alum-(K)			×	×	
Alunogen			×	×	
Anhydrite				×	
Copiapite group	×	×	×	×	×
Coquimbite			×	×	
Epsomite			×	×	
Fibroferrite			×		
Giacovazzoite				×	
Goldichite				×	
Gypsum	×		×	×	×
Halotrichite	×		×	×	
Jarosite subgroup	×		×	×	×
Khademite				×	
Krausite			×	×	
Magnanelliite				×	
Melanterite	×	×	×	×	×
Pickeringite			×		
Rhomboclase			×		
Römerite			×	×	
Scordariite				×	
Volaschioite			×		
Voltaite			×	×	
Wilcoxite			×		

Note: BdV = Buca della Vena mine; CdR = Canale della Radice mine; For = Fornovolasco mine; MA = Monte Arsiccio mine; Pol = Pollone mine. Crosses indicate that the mineral has been identified in the corresponding locality. Copiapite group and jarosite subgroup minerals have not been fully characterized from all the occurrences and consequently they are reported as unspecified members of their own group or subgroup.

3.1. Alum-(K)

Alum-(K), ideally $KAl(SO_4)_2(H_2O)_{12}$, is a common sulfate first described by Pliny the Elder in 77 CE [13] and typically represents the result of the action of H_2SO_4 formed during the weathering of sulfides (mainly pyrite) on (K,Al)-rich silicate rocks or it forms through the action of S-bearing vapors in fumaroles [14]. It belongs to the alum group, a series of minerals and synthetic compounds having cubic symmetry and general formula $X^+Y^{3+}(T^{6+}O_4)_2(H_2O)_{12}$. In natural phases, T = S. In addition to alum-(K), natural members of this group are alum-(Na) (X = Na, Y = Al), lanmuchangite (X = Tl, Y = Al), tschermigite ($X = NH_4$, Y = Al), and possibly lonecreekite ($X = NH_4$, Y = Fe).

In the secondary assemblages from the Apuan Alps, the occurrence of alum-(K) was reported by D'Achiardi [1] from the Valdicastello mines, but no further data were given. The first modern report is from the Fornovolasco mine, where it occurs as granular colorless anhedral grains, some mm in size, or as very rare octahedral individuals, up to 5 mm in size, associated with römerite, halotrichite, copiapite, and voltaite (Figure 2); alunogen and krausite were only once observed in association with alum-(K). A full crystal-chemical characterization of this sample of alum-(K) was given by Biagioni et al. [15]. A peculiar feature of the studied material is the occurrence of detectable amount of Tl; in addition, the presence of (NH_4), hypothesized on the basis of some crystal-chemical features, was confirmed through Fourier-transform infrared (FTIR) spectroscopy. Moreover, minor Fe^{3+} replaces Al^{3+}, with a Fe/(Fe + Al) atomic ratio close to 0.15, as indicated by the electron microprobe data and confirmed through crystal structure refinement based on single-crystal X-ray diffraction (SC-XRD) data. Taking into account chemical, spectroscopic, and structural data, the population $[K_{0.74}(NH_4)_{0.16}Tl_{0.10}]$ was proposed for the K site of alum-(K). The content of Tl^+ and $(NH_4)^+$, both having an ionic radius larger than that of K^+, results in some peculiar features of the sample from Fornovolasco. In alum-(K), SO_4 groups usually display a positional disorder that can be expressed through the disorder parameter *k* (that is inversely related to the degree of disorder—see, for instance [16]); in this sample, the *k* value is

ca. 0.77 and this high value is confirmed also through micro-Raman spectroscopy [15]. Another feature is the expansion of the unit-cell parameter, a = 12.2030(2) Å, larger than that reported for synthetic $KAl(SO_4)_2(H_2O)_{12}$, i.e., a = 12.1640(5) Å [17]. Biagioni et al. [15] also investigated the local environment of Tl hosted in alum-(K) through X-ray Absorption Spectroscopy (XAS), showing that Tl^+ has a first coordination shell formed by 6 O atoms at 2.84(2) Å.

Figure 2. Alum-(K) from the Fornovolasco mine, as octahedral colorless crystals up to 5 mm in size, with brown römerite and acicular crystals of halotrichite.

Alum-(K) has also been identified in the sulfate assemblage from the Monte Arsiccio mine. At this locality, alum-(K) is very common and occurs as granular aggregates of colorless anhedral individuals or, rarely, as well-developed octahedra, up to 3–4 mm in size (Figure 3). It is associated with melanterite, halotrichite, alunogen, krausite, coquimbite, römerite, copiapite, and voltaite. Chemically, K, Al, S, and minor Fe were detected through qualitative EDS analyses. This result was confirmed through the refinement of the crystal structure using SC-XRD data, showing negligible Tl contents and a Fe/(Fe + Al) atomic ratio close to 0.20. The very low amount of Tl and the virtual absence of (NH_4), as indicated by FTIR data [18], agrees with the smaller unit-cell parameter a = 12.1693(5) Å, and the lower value of the k parameter (ca. 0.71), thus indicating a higher degree of positional disorder of the SO_4 groups with respect to the Fornovolasco sample. Alum-(K) from Monte Arsiccio is typically associated with the new phases giacovazzoite, scordariite, and magnanelliite, and it occurs also with krausite; likely these new mineral species may be the result of the alteration of alum-(K) (e.g., [4]).

Figure 3. Alum-(K) from the Monte Arsiccio mine, as yellowish octahedra up to 2 mm in size.

3.2. Alunogen

Alunogen, ideally $Al_2(SO_4)_3(H_2O)_{12}\cdot 5H_2O$, is another common sulfate deriving through the action of H_2SO_4 formed during the weathering of sulfides on Al-bearing silicate rocks (e.g., [19]). This mineral was identified only at the Fornovolasco and Monte Arsiccio mines.

At Fornovolasco, alunogen is very rare and it was identified on the basis of EDS chemical data, showing Al:S atomic ratios close to 2:3, and on the basis of the tabular morphology. Indeed, it was observed only once as μm-sized tabular crystals, associated with voltaite (Figure 4).

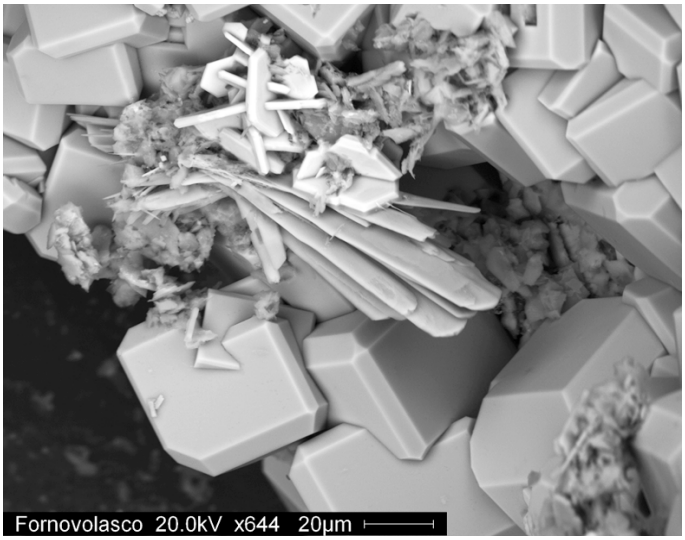

Figure 4. Alunogen from the Fornovolasco mine, as tabular crystals associated with voltaite, in cubic individuals, and an unknown tabular phase, bright in back-scattered electrons.

Figure 5. Alunogen from the Monte Arsiccio mine, as white fibrous aggregates formed by tabular individuals, up to 4 cm long.

Alunogen is relatively common at the Monte Arsiccio mine, where it occurs as cm-thick fibrous veins, composed by tabular crystals characterized by a perfect {010} cleavage. In the studied specimens, this mineral is associated with coquimbite, halotrichite, and krausite (Figure 5). SC-XRD data collected on the Monte Arsiccio sample gave the following unit-cell parameters: a = 7.4186(7), b = 26.986(2), c = 6.0526(6) Å, α = 89.9740(10), β = 97.556(6), γ = 91.880(6)°, space group P-1. These values can be compared with those reported by Menchetti and Sabelli [20] [a = 7.425(2), b = 26.975(2), c = 6.0608(5) Å, α = 90.03(1), β = 97.66(2), γ = 91.94(1)°] and Fang and Robinson [21] [a = 7.420(6), b = 26.97(2), c = 6.062(5) Å, α = 89.95(8), β = 97.57(8), γ = 91.88(8)°]. The refinement of the crystal structure of

the sample from the Monte Arsiccio mine [R_1 = 0.090 for 2797 reflections with $F_o > 4\sigma(F_o)$] led to the formula $Al_2(SO_4)_3(H_2O)_{12}\cdot 4.5H_2O$ for the studied material, in agreement with previous studies on alunogen, e.g., [20,21].

3.3. Anhydrite

Anhydrite, ideally $CaSO_4$, has been identified only once, in a specimen from the Monte Arsiccio mine. It occurs as prismatic crystals, up to 0.2 mm, associated with halotrichite, magnanelliite, and voltaite. Its identification is based on SC-XRD data and micro-Raman spectroscopy. The refinement of unit-cell parameters gave a *C*-centered cell with $a = 6.234(5)$, $b = 6.989(5)$, $c = 6.992(4)$ Å. The occurrence of anhydrite in sulfate assemblages originating from pyrite oxidation is rare, even if it was previously reported by other authors (e.g., [19,22]).

3.4. Copiapite Group Minerals

Copiapite group minerals are among the most common iron sulfates occurring as alteration products of sulfide deposits and mine-wastes [23]. Their general formula can be written as $AR^{3+}{}_4(SO_4)_6(OH)_2(H_2O)_{14}\cdot 6H_2O$, where A = Fe^{2+}, 2/3Fe^{3+}, 2/3Al, Mg, Zn, Cu^{2+}, Ca and R = Fe^{3+}, Al [23]. A review of previous chemical and crystallographic studies of the copiapite group minerals can be found in [24]. Recent contributions to the crystal chemistry of the copiapite group minerals were given in [25,26], where two structural kinds (named MG- and AL-type, respectively) are distinguished based on the orientation of the $A(H_2O)_6$ octahedra and the topology of the infinite chains occurring in the crystal structures of copiapite group minerals.

The first occurrence of copiapite group minerals from the Apuan Alps was reported by Biagioni et al. [27] from the Fornovolasco mine. Here, copiapite group minerals occur as microcrystalline aggregates, formed by thin tabular canary-yellow crystals, closely associated with halotrichite, melanterite, and römerite (Figure 6a,b). Later, Mauro et al. [28] described the presence of magnesiocopiapite from another sulfate assemblage from the same locality. This mineral occurs as flower-like aggregates composed by micaceous crystals, yellow in color, associated with an intermediate member of the halotrichite-pickeringite series. Chemical analyses led to the empirical formula $Mg_{1.29}(Fe^{3+}{}_{3.84}Al_{0.11})_{\Sigma 3.95}(S_{5.93}O_{24})(OH)_2\cdot 20H_2O$, in agreement with the end-member formula of magnesiocopiapite, i.e., $MgFe^{3+}{}_4(SO_4)_6(OH)_2\cdot 20H_2O$ [28]. In addition, a copiapite group mineral was collected in association with römerite, as spheroidal cm-sized aggregates, formed by thin tabular crystals. Notwithstanding the very small size and the low diffraction quality of the available material, unit-cell parameters were measured using a ~ 0.06 × 0.04 × 0.01 mm crystal through SC-XRD, resulting in the following values: a = 7.349(5), b = 7.384(5), c = 18.784(14) Å, α = 91.73(2), β = 98.72(2), γ = 102.253(18)°. The crystal structure was refined. Whereas the final R factor was very high (R_1 = 0.20), the observed geometrical features were physically sound, and the high R factor was mainly due to the weakness of the observed reflections. The formula derived through the crystal structure refinement is $(Mg_{0.83}Fe^{2+}{}_{0.17})Fe^{3+}{}_4(SO_4)_6(OH)_2(H_2O)_{14}\cdot 6H_2O$, allowing the classification of this sample as magnesiocopiapite. A structural feature confirming the Mg-rich nature of the studied specimen is represented by the orientation of the isolated $A(H_2O)_6$ octahedra and the topology of the infinite chains forming its crystal structure, agreeing with the MG-type (according to [26]). The unit-cell volume of this structural type is larger than that shown by AL-copiapites and the measured unit-cell volume of the sample from Fornovolasco (i.e., 982.5(12) $Å^3$) can be compared with that of the synthetic analogue of magnesiocopiapite, i.e., 983.6(1) $Å^3$ [26].

Copiapite group minerals were reported in the other pyrite ± baryte ± iron oxide deposits [29], but no mineralogical data are available. Some data have been collected only on a sample of copiapite group minerals from the Monte Arsiccio mine. In the studied sample, this mineral occurs as microcrystalline aggregates, up to some cm in size, canary-yellow in color, formed by thin tabular individuals, up to 100 μm in size, associated with halotrichite, römerite, and krausite (Figure 6c). Unit-cell parameters, refined from SC-XRD data, are a = 7.354(2), b = 7.388(2), c = 18.799(6) Å,

α = 91.253(11), β = 98.882(10), γ = 102.188(9)°. The R_1 factor was slightly better than that obtained for the Fornovolasco sample [R_1 = 0.135 for 1668 reflections with $F_o > 4\sigma(F_o)$] and supported the crystal-chemical formula $(Mg_{0.77}Fe^{2+}_{0.23})Fe^{3+}_4(SO_4)_6(OH)_2(H_2O)_{14}\cdot 6H_2O$. Consequently, also the copiapite group mineral from the Monte Arsiccio mine can be classified as magnesiocopiapite. Again, structural features corresponding to the MG-type as well as the unit-cell volume [984.9(5) Å^3] agree with this identification.

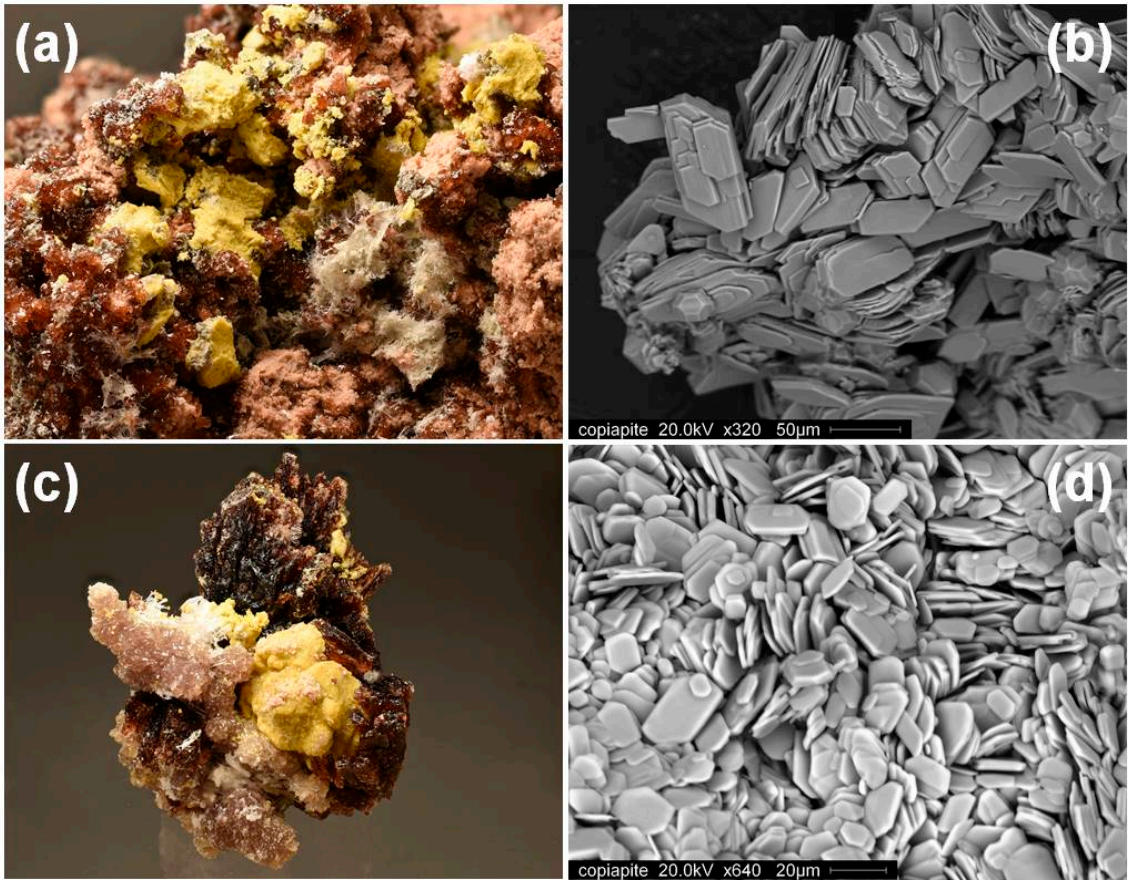

Figure 6. Copiapite group minerals from the pyrite ores of the Apuan Alps. (**a**) Magnesiocopiapite, as microcrystalline canary-yellow masses up to 5 mm across, with brown römerite and hairy halotrichite from the Fornovolasco mine. (**b**) Details of the crystal morphology of magnesiocopiapite from the previous locality. (**c**) Magnesiocopiapite, as rounded aggregates of canary-yellow microcrystals, up to 1 cm across, associated with krausite, halotrichite, and römerite, from the Monte Arsiccio mine. (**d**) A copiapite group mineral from the Pollone mine, as micrometer-sized tabular crystals.

Owing to the common presence of copiapite group minerals in several sulfate assemblages from the Apuan Alps (Figure 6d), further data have to be collected in order to achieve a full characterization of these phases.

3.5. Coquimbite

Coquimbite, ideally $AlFe^{3+}_3(SO_4)_6(H_2O)_{12}\cdot 6H_2O$, is an Al-$Fe^{3+}$ hydrated sulfate recently redefined by Mauro et al. [30]. The occurrence of this mineral in the secondary assemblages of the pyrite ores from the Apuan Alps was first hypothesized by D'Achiardi [1]. However, no data were reported.

The first identification was performed in the Fornovolasco mine, where coquimbite occurs as pseudohexagonal bipyramidal crystals, less than 50 µm in size, associated with römerite (Figure 7). It was identified through an X-ray powder diffraction (XRPD) pattern collected using a 114.6 mm

Gandolfi camera and Ni-filtered Cu$K\alpha$ radiation. EDS chemical analyses pointed to an Al/(Fe + Al) atomic ratio of ~0.20, close to the ideal ratio 0.25.

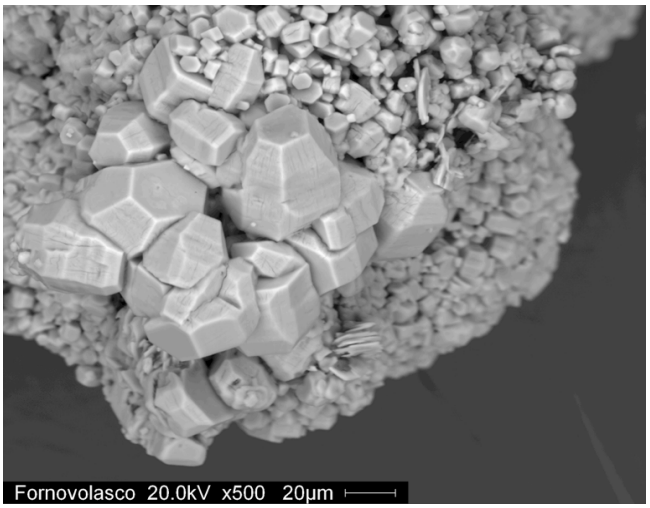

Figure 7. Coquimbite from the Fornovolasco mine, as pseudohexagonal bipyramidal crystals.

Coquimbite has been reported also from the Monte Arsiccio mine, where this sulfate forms purple pseudohexagonal crystals, up to 3 cm in size, associated with alunogen, halotrichite, khademite, krausite, melanterite, and römerite (Figure 8). Chemical analyses, performed through WDS mode, gave the following chemical formula: $Al_{0.96}Fe_{3.11}S_{5.97}O_{24}{\cdot}18H_2O$ [30], in agreement with the ideal formula. Unit-cell parameters, refined using SC-XRD data, are a = 10.9318(12), c = 17.069(2) Å, space group P-31c [30]. Mauro et al. [30] discussed also the infrared and micro-Raman spectral features of coquimbite.

Figure 8. Coquimbite from the Monte Arsiccio mine, as purple pseudohexagonal prismatic crystals, up to 1.5 cm across.

3.6. Epsomite

Epsomite, ideally $Mg(SO_4)(H_2O)_6{\cdot}H_2O$, belongs to a series of orthorhombic sulfates, along with its Zn-isotype goslarite and the Ni-isotype morenosite [23]. It is a relatively common mineral occurring in several geological environments, such as the oxidation zone of sulfidic ore deposits hosted in Mg-rich rocks (e.g., dolostone). Since pyrite ores from the Apuan Alps are, at some localities, located close to the

contact between phylladic rocks and metadolostone, epsomite is a rather common mineral. Currently, it has been identified in two localities: the Fornovolasco and the Monte Arsiccio mines.

At Fornovolasco, epsomite occurs in sulfate piles occurring in the 740 m level (one of the oldest tunnels of the mining complex), along with an intermediate member of the halotrichite-pickeringite series, melanterite, gypsum, magnesiocopiapite, and wilcoxite [28]. It usually forms anhedral, colorless, grains or prismatic individuals, whereas thin needles, up to 3 cm in length, are rarer (Figure 9). Chemical analysis (performed in EDS mode) showed Mg, S, and minor Fe as the only elements with $Z > 8$ above the detection limit. This result was confirmed by the crystal structure refinement that pointed to a chemical composition $(Mg_{0.74}Fe_{0.16})(SO_4)(H_2O)_6 \cdot H_2O$ [28]. Unit-cell parameters, refined from SC-XRD data, are a = 11.8664(3), b = 12.0150(3), c = 6.8598(2) Å, space group $P2_12_12_1$ [28].

Figure 9. Epsomite from the Fornovolasco mine as hairy acicular crystals, up to 2 cm long, and microcrystalline sugary colorless aggregates.

At the Monte Arsiccio mine epsomite was identified as whitish efflorescences or very thin colorless needles, associated with gypsum, likely resulting from the interaction between H_2SO_4 (released from pyrite oxidation) and metadolostone. Its identification was confirmed through EDS qualitative data and XRPD data collected using a 114.6 mm Gandolfi camera and Ni-filtered Cu$K\alpha$ radiation.

3.7. Fibroferrite

Fibroferrite is a complex hydrated Fe^{3+} sulfate, ideally $Fe^{3+}(SO_4)(OH)(H_2O)_2 \cdot 3H_2O$, and can be the result of the oxidation of melanterite [31]. This mineral was found as fine-fibrous crusts, with a silky luster, greyish-white in color (Figure 10), in the Fornovolasco mine, in close association with melanterite, as revealed by an XRPD pattern collected using a 114.6 mm Gandolfi camera and Ni-filtered Cu$K\alpha$ radiation. Qualitative EDS chemical analyses showed Fe and S as the only elements with $Z > 8$ above the detection limit. The identification of fibroferrite was further confirmed through micro-Raman spectroscopy.

3.8. Giacovazzoite

Giacovazzoite, ideally $K_5Fe^{3+}{}_3O(SO_4)_6(H_2O)_9 \cdot H_2O$, is a new species recently discovered at the Monte Arsiccio mine, sharing some structural relationships with metavoltine-group minerals [4]. Indeed, it displays a $[Fe^{3+}{}_3O(SO_4)_6(H_2O)_3]^{5-}$ cluster, occurring also in metavoltine and related compounds [32]. Giacovazzoite occurs as prismatic crystals, orange-brown in color, up to 0.1 mm in size, with a vitreous luster (Figure 11). It shows a perfect {100} cleavage. It is associated with alum-(K), gypsum, krausite, magnanelliite, and scordariite. The crystallographic investigation of

giacovazzoite revealed its isotypic relationship with the synthetic β-Maus's salt described in [33]. Unit-cell parameters are a = 9.4797(2), b = 18.4454(5), c = 18.0540(4) Å, β = 92.626(2)°, space group $P2_1/c$. The empirical chemical formula of giacovazzoite is $K_{5.06}Fe^{3+}_{2.98}O(SO_4)_{6.00}\cdot 10H_2O$, in agreement with the ideal formula [4].

Figure 10. Fibroferrite from the Fornovolasco mine, as spongy fibrous aggregates. Field of view: 4 cm.

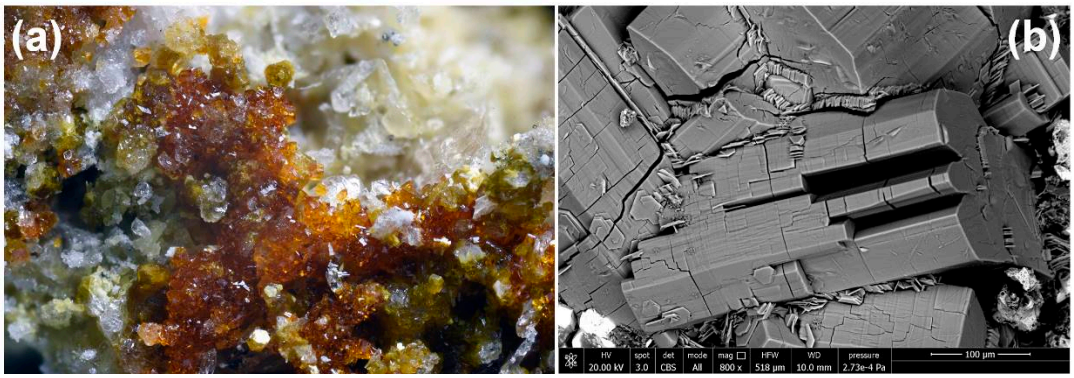

Figure 11. Giacovazzoite, as orange-brown prismatic crystals (**a**), associated with yellow-green scordariite and alum-(K). Field of view = 3 mm. A detail of the morphology of the crystals of giacovazzoite is shown in the SEM photo (**b**); thin tabular hexagonal crystals of a metavoltine-related mineral are also present.

The genesis of giacovazzoite may be related to the decomposition of Fe-rich domains of alum-(K), in agreement with the study of Mereiter and Völlenkle [33] on its synthetic analogue. Biagioni et al. [4] gave a full set of crystal-chemical data of giacovazzoite, as well as of its dehydration product.

3.9. Goldichite

Goldichite, ideally $KFe^{3+}(SO_4)_2(H_2O)_4$, is a rare sulfate found only in few localities worldwide (www.mindat.org). It commonly occurs as an oxidation product of sulfide ores [34] or as fumarolic sublimate [35,36]. In the studied localities, goldichite has been identified only at the Monte Arsiccio mine where it occurs as prismatic to tabular crystals, up to 3 cm in length (Figure 12), having a morphology corresponding to that described by Rosenzweig and Gross [34] for goldichite from its type locality. Crystals can form fan-like aggregates, usually associated with halotrichite, and,

less frequently, with alum-(K), gypsum, jarosite, krausite, melanterite, and sulfur. Color is yellowish green in natural light, whereas it is lavender pink under artificial light, in agreement with [34]. The identification of goldichite was initially performed through XRPD data collected using a 114.6 mm Gandolfi camera and Ni-filtered Cu$K\alpha$ radiation. In addition, SC-XRD data were collected obtaining the following unit-cell parameters a = 10.4114(8), b = 10.4809(7), c = 9.1079(7) Å, β = 101.67(3)°, space group $P2_1/c$. The crystal structure was refined down to an agreement factor R_1 = 0.0437 for 3187 reflections with $F_o > 4\sigma(F_o)$, and shows the same crystallographic features described by previous investigators [37,38].

Figure 12. Goldichite, purple prismatic crystals, up to 2 cm in length, associated with fibrous halotrichite, from the Monte Arsiccio mine.

3.10. Gypsum

Gypsum is a common mineral in secondary assemblages formed through sulfide oxidation, and it was reported from the pyrite deposits occurring close to the Valdicastello Carducci village by D'Achiardi [1]. Indeed, at the Pollone and Monte Arsiccio mines, gypsum is very common in the old mining works, where it covers the tunnel walls and forms aggregates of tabular crystals, up to more than 1 cm in size (e.g., [29]). In addition, gypsum was identified as rare individuals in the complex sulfate assemblage from the Monte Arsiccio mine, closely associated with goldichite and alum-(K). Its identification was based on SC-XRD, giving unit-cell parameters a = 6.2853(6), b = 15.2092(13), c = 5.6774(5) Å, β = 114.077(2)°, space group $C2/c$.

Biagioni et al. [27] described the occurrence of gypsum in the Fornovolasco mine, as colorless to light yellow tabular crystals, up to 5 mm in size. This sulfate was relatively common in association with epsomite and other Mg-rich sulfates, formed through the interaction between H_2SO_4 and metadolostone. Another occurrence of gypsum was reported from the Buca della Vena mine, where this sulfate occurs in association with some iron phosphate-sulfates (i.e., destinezite, bohuslavite [3,29]). The identification of gypsum in these occurrences is supported by XRPD patterns and EDS analyses.

3.11. Halotrichite Group Minerals

Minerals belonging to the halotrichite group, having general formula $A^{2+}B^{3+}{}_2(SO_4)_4(H_2O)_{17}{\cdot}5H_2O$, are common phases in secondary mineral assemblages from sulfide ore occurrences [22]. Halotrichite (A = Fe, B = Al) and pickeringite (A = Mg, B = Al) are the most common species of the halotrichite group.

The first description of halotrichite from the Apuan Alps was reported by D'Achiardi [1], who cited the presence of this mineral in the pyrite ores close to the Valdicastello Carducci village, on the basis of qualitative chemical data and physical properties.

Biagioni et al. [27] reported the occurrence of halotrichite from the Fornovolasco mine, using XRPD data and qualitative EDS chemical analyses. Halotrichite occurs as white acicular crystals, up to 2 cm in length, or as fibrous masses, associated with melanterite, a copiapite group mineral, römerite, and voltaite (Figure 13). Later, Mauro et al. [28] described the occurrence of intermediate members of the halotrichite-pickeringite series, as hairy whitish needles, or as rounded aggregates of thin acicular crystals. Chemical data, performed through EDS mode, indicated compositions very close to the boundary between halotrichite and pickeringite.

Figure 13. Halotrichite, as hairy acicular crystals, up to 7 mm in length, with römerite, greenish voltaite, and a tertiary copiapite group mineral from the Fornovolasco mine.

In addition, halotrichite was identified in the sulfate assemblage from the Monte Arsiccio mine (Figure 14), as cm-sized tufts of thin needles, whitish to greenish in color, in some cases embedding euhedral individuals of other sulfates (e.g., coquimbite, goldichite, voltaite). The identification is based on XRPD patterns, collected through a 114.6 mm Gandolfi camera and Ni-filtered Cu$K\alpha$ radiation, and EDS analyses, showing Fe, Al, and S as the only elements with $Z > 8$ above the detection limit. Finally, thin needles of an halotrichite group mineral were identified through micro-Raman spectroscopy at the Buca della Vena mine, in close association with melanterite.

Figure 14. Halotrichite, as hairy acicular crystals, up to 15 mm, from the Monte Arsiccio mine.

3.12. Jarosite Subgroup Minerals

Minerals belonging to the alunite supergroup have the general chemical formula $DG_3(TX_4)_2X'_6$ [39]. Jarosite subgroup minerals are characterized by G = Fe^{3+}, T = S^{6+}, X = O^{2-}, and X′ = $(OH)^-$, and they are common in different geological environments, among which oxidized sulfide ores [40,41]. Following [39], phases with D = Ag (argentojarosite), H_3O (hydroniumjarosite), K (jarosite), Na (natrojarosite), NH_4 (ammoniojarosite), Tl (dorallcharite), and Pb (plumbojarosite) are known.

The first report of jarosite subgroup minerals from the Apuan Alps was given by Senesi [42] from the Pollone mine, where this phase is intimately associated with a REE-bearing phosphate, tentatively classified as florencite-(Ce), and strengite. Although jarosite subgroup minerals are likely widespread in all the pyrite ores from the southern Apuan Alps, few data are currently available, mainly owing to their microcrystalline nature. Jarosite subgroup minerals were identified in three other mining sites: Buca della Vena, Fornovolasco, and Monte Arsiccio.

At the Monte Arsiccio mine, a jarosite subgroup mineral is rather widespread as yellowish microcrystalline coatings on the tunnel walls, associated with biofilms composed by bacterial colonies; this phase is slightly enriched in Tl [9] but no quantitative crystal-chemical data are currently available. In addition, jarosite was identified as microcrystalline aggregates of orange rhombohedral individuals, up to 10 μm in size, associated with other phases (e.g., melanterite, goldichite, krausite, magnanelliite). Its EDS chemical analysis showed the occurrence of K, Fe, and S as the only elements with $Z > 8$, giving the chemical formula $K_{0.80}Fe_{2.78}S_{2.14}O_8(OH)_6$, in agreement with the ideal stoichiometry $KFe_3(SO_4)_2(OH)_6$. XRPD patterns, collected through a 114.6 mm Gandolfi camera and Ni-filtered Cu$K\alpha$ radiation, and micro-Raman spectroscopy, further supported this identification. Unit-cell parameters, refined from 21 unequivocally indexed reflections using the software UnitCell [43], are a = 7.3071(6), c = 17.1884(16) Å.

Fewer data are currently available for the other two occurrences. At Fornovolasco, a jarosite subgroup mineral was observed as μm-sized rhombohedral crystals, brownish in color, on a deeply oxidized surface of pyrite. Its EDS chemical analysis revealed the occurrence of Fe and S, with the typical Fe/S atomic ratio of 3:2. No other elements with $Z > 8$ were detected, suggesting that the studied sample could be ammoniojarosite or hydroniumjarosite. Following Sasaki et al. [44], micro-Raman spectroscopy could be used for discriminating jarosite subgroup minerals from each other. In particular, these authors observed that some Raman bands are correlated with the length of the unit-cell parameter c, the latter being related to the ionic radius of the D chemical component in the formula of these minerals. Ammoniojarosite and hydroniumjarosite have significantly different values of the unit-cell parameters c, i.e., c = 17.53 [45] and 16.99 Å [46], respectively. Plášil et al. [47] gave a c parameter of 17.05 Å for natural hydroniumjarosite. Following Sasaki et al. [44], these two phases may be distinguished on the basis of the Raman shift of several bands. Data collected on the sample from Fornovolasco agrees with a c parameter closer to ~17 Å than 17.5 Å, thus supporting the identification as hydroniumjarosite. However, some differences in the O–H stretching and bending regions [47,48] may suggest that more data would be necessary for a correct classification of this jarosite subgroup mineral.

At Buca della Vena mine, a jarosite subgroup mineral was identified through micro-Raman spectroscopy as aggregates of μm-sized equant orange individuals on schist, in association with bohuslavite and gypsum. Chemical data are currently lacking, whereas its Raman spectrum is very similar to that of the sample from Monte Arsiccio, suggesting it could be classified as jarosite.

3.13. Khademite

Khademite is a relatively rare fluo-sulfate with ideal composition $Al(SO_4)F(H_2O)_5$, whose troubled definition has been recently reviewed by Košek et al. [49]. In the secondary assemblages from the pyrite ores of the Apuan Alps, khademite was identified as colorless to whitish tabular crystals (Figure 15), up to 5 mm in size, associated with coquimbite, halotrichite, and krausite, in the sulfate assemblage from the Monte Arsiccio mine [50]. Chemical analysis pointed to the formula $Al_{0.96}S_{1.02}O_4[F_{0.84}(OH)_{0.16}]\cdot 5H_2O$. Unit-cell parameters, refined through SC-XRD data, are a = 11.1713(2), b = 13.0432(3), c = 10.8815(2),

space group *Pcab* [50]. Khademite is the second fluo-sulfate identified in the sulfate assemblages from the Apuan Alps and it was fully characterized through SC-XRD and micro-Raman spectroscopy by Mauro et al. [50].

Figure 15. Khademite, colorless tabular crystals up to 3 mm with tufts of white halotrichite on krausite from the Monte Arsiccio mine.

3.14. Krausite

Krausite, ideally $KFe^{3+}(SO_4)_2(H_2O)$, is one of the few mineral species belonging to the quaternary system K_2O–Fe_2O_3–SO_3–H_2O and it occurs as an uncommon phase in sulfate-bearing assemblages (e.g., [22]), in some cases occurring also in fumarolic environments (e.g., [36]).

The first report of krausite from the pyrite ores of the Apuan Alps was given by Mauro [51] from the Fornovolasco mine, where this mineral was identified on the basis of qualitative EDS chemical analyses and an XRPD pattern collected using a 114.6 mm Gandolfi camera and Ni-filtered Cu$K\alpha$ radiation. Krausite occurs as rosettes composed by thin tabular colorless crystals, less than 50 μm in length, associated with voltaite, alunogen and alum-(K) (Figure 16).

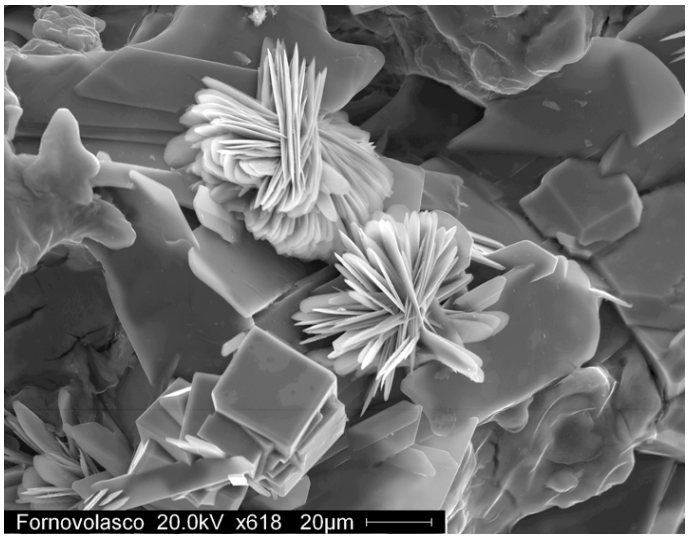

Figure 16. Krausite from the Fornovolasco mine, as rosettes of tabular crystals with alunogen and cubic voltaite.

A more abundant finding was recently reported from the Monte Arsiccio mine [30], where krausite is common and occurs as well-developed euhedral crystals, showing different morphologies. Commonly, it forms spheroidal aggregates, up to 15 mm in diameter, associated with halotrichite; in addition, it forms rounded aggregates of tabular individuals, up to 1 cm. Color is green in natural light, whereas it is pinkish under artificial light. Krausite is typically grown on coquimbite or römerite (Figure 17) or it is embedded in fibrous halotrichite. Other associated phases are alum-(K), alunogen, goldichite, khademite, magnanelliite, and magnesiocopiapite. Chemical data, collected through WDS mode, pointed to the formula $K_{1.00}Fe_{1.01}(SO_4)_2(H_2O)$, in agreement with the ideal one. SC-XRD gave the unit-cell parameters a = 7.9077(3), b = 5.1458(2), c = 9.0119(4) Å, β = 102.802(2)°, space group $P2_1/m$. The results of the crystal structure refinement [R_1 = 0.0200 for 1466 reflections with $F_o > 4\sigma(F_o)$] agree with previous structural studies [52,53].

Figure 17. Krausite from the Monte Arsiccio mine, as aggregates of tabular crystals, up to 1 cm, with violet coquimbite and brown römerite.

Figure 18. Magnanelliite, aggregates of prismatic yellow crystals, up to 0.5 mm, grown on alum-(K), from the Monte Arsiccio mine.

3.15. Magnanelliite

Magnanelliite, $K_3Fe^{3+}{}_2(SO_4)_4(OH)(H_2O)_2$, is a recent addition to the sulfate systematics after its discovery at the Monte Arsiccio mine by Biagioni et al. [6]. It occurs as prismatic crystals, steeply terminated, up to 1 mm in length, occurring as isolated individuals or as divergent intergrowths (Figure 18). Color ranges from light yellow to orange. Magnanelliite is typically associated with other K-sulfates and, in particular, with alum-(K) and krausite. In addition, it has been observed in association with anhydrite, giacovazzoite, gypsum, halotrichite, jarosite, melanterite, scordariite, and voltaite. Its empirical formula is $(K_{2.98}Na_{0.04})_{\Sigma 3.02}(Fe^{3+}{}_{2.08}Al_{0.05}Mg_{0.01})_{\Sigma 2.14}S_{3.93}O_{16}(OH)(H_2O)$. Unit-cell parameters are a = 7.5491(3), b = 16.8652(6), c = 12.1574(4) Å, β = 94.064(1)°, space group $C2/c$ [6]. Magnanelliite is the Fe^{3+}-analogue of alcaparrosaite, ideally $K_3Ti^{4+}Fe^{3+}(SO_4)_4O(H_2O)_2$ [54].

3.16. Melanterite

Melanterite is the first oxidation product of iron sulfides and it is very common in all secondary sulfate assemblages. Its occurrence from the Apuan Alps has been reported since a long time. For instance, the Tuscan naturalist Giovanni Targioni Tozzetti described its presence in the old tunnels of the Canale della Radice mine [55], whereas D'Achiardi [1] reported the occurrence of this mineral in several localities (Valdicastello, Canale della Radice).

The first modern identification was performed by Biagioni et al. [27] from the Fornovolasco mine, as greenish fibrous aggregates, up to 1 cm in size, associated with pyrite, römerite, and, more rarely, with fibroferrite. These specimens were later studied by Mauro et al. [56] who reported WDS chemical data, giving the formula $(Fe_{0.95}Mg_{0.06})_{\Sigma 1.01}SO_4{\cdot}7H_2O$. Unit-cell parameters are a = 14.075(8), b = 6.5014(4), c = 11.0426(6) Å, β = 105.632(3)°, space group $P2_1/c$. Structural details (including H-bonding) and micro-Raman spectroscopic features are discussed in Mauro et al. [56]. Melanterite was reported also from the Pollone, Monte Arsiccio, and Buca della Vena mines [29]. EDS chemical data are available only for the Monte Arsiccio sample, and show a Fe:S ratio close to 1, in agreement with the ideal stoichiometry. No chemical and crystallographic data are available for the other occurrences, where the presence of melanterite was confirmed through XRPD patterns and micro-Raman spectroscopy.

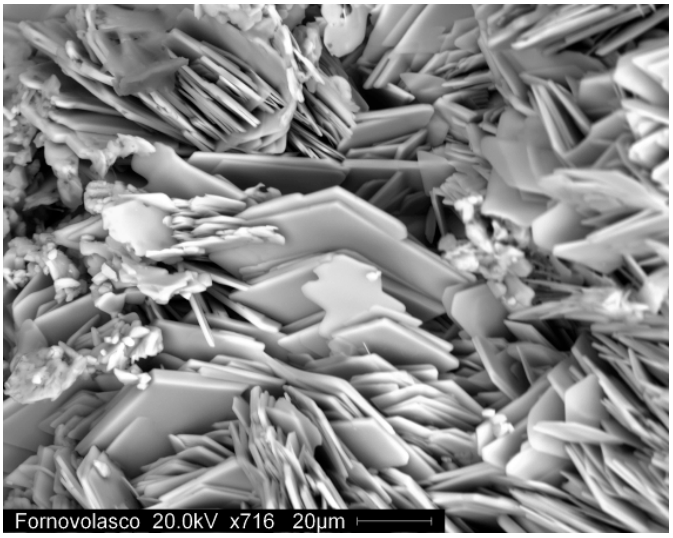

Figure 19. Rhomboclase, rhombic tabular crystals from the Fornovolasco mine.

3.17. Rhomboclase

Rhomboclase, ideally $(H_5O_2)Fe^{3+}(SO_4)_2(H_2O)_2$, is a relatively frequent iron sulfate occurring in oxidized sulfide deposits [23]. In the Apuan Alps, this phase was identified only once in the Fornovolasco mine, as aggregates of thin tabular rhombic crystals, less than 100 µm in size (Figure 19).

Chemical data, collected through EDS mode, gave an Fe:S atomic ratio of 0.5, in agreement with the stoichiometry of rhomboclase; the identification was further supported by an XRPD pattern collected using a 114.6 mm Gandolfi camera and Ni-filtered Cu$K\alpha$ radiation [51].

3.18. Römerite

Römerite is a mixed divalent-trivalent iron sulfate, ideally $Fe^{2+}Fe^{3+}{}_2(SO_4)_4(H_2O)_{14}$, typically observed in sulfate deposits and as oxidation product of sulfide ores [23]. Along with lishizhenite, $ZnFe^{3+}{}_2(SO_4)_4(H_2O)_{14}$, it forms the römerite group.

The first description of römerite from the Apuan Alps pyrite ores was reported by Biagioni et al. [27] from the Fornovolasco mine, as microcrystalline pinkish aggregates or as euhedral prismatic individuals, up to 3 mm in size (Figure 20). In the studied specimens, this mineral is usually associated with halotrichite, magnesiocopiapite, and melanterite; rarely, alum-(K), alunogen, coquimbite, and voltaite can also occur. The samples from Fornovolasco were crystal-chemically characterized by Mauro et al. [57]. Chemical analysis, performed using WDS mode, gave the chemical formula $(Fe^{2+}{}_{0.82}Mg_{0.22})_{\Sigma 1.04}Fe^{3+}{}_{2.08}S_{3.95}O_{16}\cdot 14H_2O$ [57], showing a minor replacement of Fe^{2+} by Mg, in agreement with the possible occurrence of the Mg-analogue of römerite, reported as the unnamed mineral UM1968-03-SO:FeHMg [58]. Unit-cell parameters, refined from SC-XRD data, are a = 6.4512(6), b = 15.323(2), c = 6.3253(6) Å, α = 90.131(5), β = 100.900(4), γ = 85.966(4)°, space group P-1 [57]. Structural details, including the H-bond system, and micro-Raman spectral features are discussed in Mauro et al. [57].

Figure 20. Römerite, prismatic crystals up to 1.5 mm with acicular crystals of halotrichite from the Fornovolasco mine.

A new finding of römerite was performed in the Monte Arsiccio mine, where this sulfate occurs as cm-thick veins, formed by brown tabular crystals, up to 3 cm in length. In these veins, some cavities are filled by euhedral individuals of römerite, associated with acicular crystals of halotrichite, canary-yellow microcrystalline aggregates of magnesiocopiapite, and rounded aggregates of tabular crystals of krausite (Figure 21). Römerite is overgrown by coquimbite, that in some cases shows some inclusions of this mixed divalent-trivalent iron sulfate. Römerite was also observed in granular aggregates, formed by prismatic crystals, having a more equant habit, up to 2 mm in size, associated with halotrichite, voltaite and krausite. The identification of römerite was confirmed through SC-XRD, giving the following unit-cell parameters: a = 6.4593(6), b = 15.3310(13), c = 6.3279(5) Å, α = 90.107(3), β = 100.948(3), γ = 85.818(3)°, space group P-1.

Figure 21. Römerite, prismatic crystals up to 1 cm with acicular crystals of halotrichite from the Monte Arsiccio mine.

Figure 22. Scordariite, as yellowish tabular pseudohexagonal crystals, up to 1 mm, on microcrystalline alum-(K) (**a**). In (**b**), pseudohexagonal crystals of scordariite grown on alum-(K) with pyrite. Both samples are from the Monte Arsiccio mine.

3.19. Scordariite and other Metavoltine-Related Minerals

Scordariite, ideally $K_8(Fe^{3+}_{0.67}\square_{0.33})[Fe^{3+}_3O(SO_4)_6(H_2O)_3]_2(H_2O)_{11}$, is a new species recently described from the Monte Arsiccio mine [5]. This mineral occurs as pseudohexagonal {0001} tabular to prismatic crystals, up to 0.5 mm in size, yellowish to brownish in color (Figure 22). The empirical formula, based on WDS data and Mössbauer spectroscopy, allowing the determination of the Fe^{2+}: Fe^{3+} atomic ratio, is $(K_{7.50}Na_{0.34})_{\Sigma 7.84}(Fe^{3+}_{6.29}Al_{0.26}Fe^{2+}_{0.20})_{\Sigma 6.75}S_{12.02}O_{50}\cdot 17H_2O$ [5]. Unit-cell parameters, refined through SC-XRD data, are a = 9.7583(12), c = 53.687(7) Å, space group R-3 [5]. The crystal structure of scordariite is closely related with that of metavoltine, ideally $Na_6K_2Fe^{2+}[Fe^{3+}_3O(SO_4)_6(H_2O)_3]_2(H_2O)_{12}$, having cell parameters a = 9.575(5), c = 18.17(1) Å, space group P3 [59]. Indeed, both minerals have a layered structure and are characterized by the heteropolyhedral cluster $[Fe^{3+}_3O(SO_4)_6(H_2O)_3]^{5-}$ observed also in giacovazzoite [4]. Scordariite can be considered a K-homeotype of metavoltine, having

a larger unit cell, with a rhombohedral lattice, a lower hydration state and a more oxidized nature, as Fe^{2+} in metavoltine is replaced by Fe^{3+} in scordariite [5].

In addition to scordariite, other phases having similar morphologies and different XRPD patterns have been observed, but their full characterization is still lacking. Unfortunately, some of them seem to be unstable, rapidly dehydrating after few days or weeks, precluding their accurate study. For instance, yellow prisms up to 100 μm with an hexagonal outline examined through SC-XRD gave the unit-cell parameters a = 9.7218(17), c = 18.784(4) Å, space group $P6_3/m$; these values are comparable with those of the α-Maus's Salt, i.e., a = 9.71(1), c = 18.96(2) Å, space group $P6_3/m$ [60]. The refinement of the crystal structure, using the structural model of Giacovazzo et al. [60] refined to R_1 ~ 15%. Unfortunately, this potential new mineral species was unstable at room conditions and it suffered dehydration during the data collection, so far precluding its characterization and its proposal as a new mineral species.

3.20. Volaschioite

Volaschioite, ideally $Fe^{3+}{}_4(SO_4)O_2(OH)_6{\cdot}2H_2O$, was first described by Biagioni et al. [2] from the Fornovolasco mine. In hand-specimens, this mineral forms radial aggregates of bladed crystals, yellowish-orange in color, elongated on [010], up to 100 μm in length and less than 5 μm across (Figure 23). Empirical formula is $Fe^{3+}{}_{4.16}(SO_4)_{0.92}O_{2.32}(OH)_6{\cdot}2H_2O$, in agreement with the ideal one obtained through the crystal structure solution and refinement. Unit-cell parameters of volaschioite are a = 16.068(4), b = 3.058(1), c = 10.929(2) Å, β = 93.82(3)°, space group $C2/m$ [2]. Rows of continuously streaked reflections, doubling the b parameter, were observed, suggesting that the solved crystal structure is only an average structure, affected by disorder between SO_4 and H_2O groups. Similar features were reported for the copper arsenate-sulfate parnauite [61].

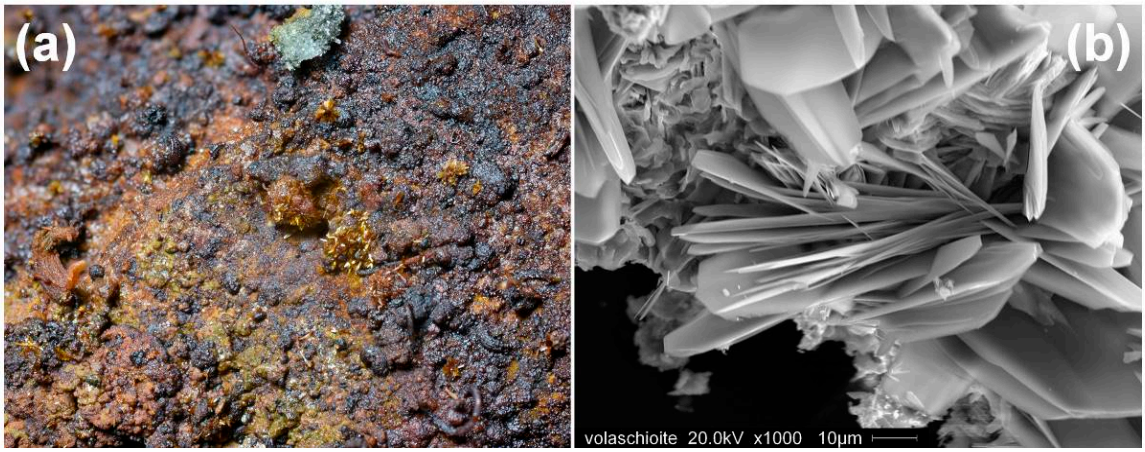

Figure 23. Volaschioite, as μm-sized yellow-orange crystals on a strongly oxidized surface (**a**) (field of view = 5 mm) and (**b**) SEM image showing the morphology of volaschioite crystals.

In holotype material, volaschioite is associated with two other unknown phases. The first one occurs as rosettes of micaceous crystals, up to 10 μm in size, containing K, Fe, S, and minor Cl as element with $Z > 8$. According to EDS data, the Fe:S ratio is close to 2. The other phase forms equant crystals, less than 5 μm in size, in which Fe and minor S and Cl were detected.

Volaschioite is the natural analogue of the phase B synthesized by Walter Lévy and Quéméneur [62] and it is chemically similar to the discredited mineral "glockerite", an ill-defined phase having a Fe:S atomic ratio of 4:1, as volaschioite. Some authors (e.g., [63,64]) suggested the identity of "glockerite" with lepidocrocite or schwertmannite.

Owing to its chemical composition similar to that of schwertmannite, volaschioite may be overlooked in several secondary assemblages, where it may be relatively common.

3.21. Voltaite

The voltaite group is formed by cubic (*Fd*-3*c*) and tetragonal ($I4_1/acd$) species having general formula $X_2Y^{2+}{}_5Z^{3+}{}_3Al(TO_4)_{12}(H_2O)_{18}$. Natural phases belonging to this group are sulfates ($T = S^{6+}$), having $Z = Fe^{3+}$. According to different combinations of X and Y cations the following species are currently known: voltaite ($X = K$, $Y = Fe^{2+}$), ammoniovoltaite ($X = NH_4$, $Y = Fe^{2+}$), magnesiovoltaite ($X = K$, $Y = Mg$), ammoniomagnesiovoltaite ($X = NH_4$, $Y = Mg$), and zincovoltaite ($X = K$, $Y = Zn$). Pertlikite, ideally $K_2(Fe^{2+},Mg)_2(Mg,Fe^{3+})_4Fe^{3+}{}_2Al(SO_4)_{12}(H_2O)_{18}$, has a tetragonal symmetry related to the ordering of divalent cations [15]. These minerals occur in oxidized ore deposits and in fumarolic environments [23].

In the Apuan Alps pyrite ores, voltaite was first reported by Biagioni et al. [27], as greenish grains or euhedral crystals characterized by the forms {100} and {110}, with minor {111} faces, green to blackish in color (Figure 24). Crystal size is usually less than 1 mm. They are usually associated with halotrichite and römerite. This material was later characterized by Biagioni et al. [15]. Crystals are chemically zoned, with at least two distinct domains having empirical chemical formulae $(K_{1.91}Tl_{0.28})_{\Sigma 2.19}(Fe^{2+}{}_{3.48}Mg_{0.95}Mn_{0.63})_{\Sigma 5.06}Fe^{3+}{}_{3.07}Al_{0.98}S_{11.92}O_{48}{\cdot}18H_2O$ and $(K_{2.04}Tl_{0.32})_{\Sigma 2.36}(Fe^{2+}{}_{3.83}Mg_{0.91}Mn_{0.29})_{\Sigma 5.03}Fe^{3+}{}_{3.05}Al_{0.97}S_{11.92}O_{48}{\cdot}18H_2O$, respectively. In addition, the occurrence of (NH_4) was revealed through FTIR spectroscopy and N was detected (but not quantified) during electron microprobe analyses [15]. The occurrence of Tl is an interesting feature of the samples of voltaite from Fornovolasco, since Tl-rich or Tl-bearing voltaites are mainly known as synthetic compounds, although previous authors described "monsmedite" [65,66], later identified as a Tl-bearing voltaite [67–69]. The presence of Tl and (NH_4) replacing K is in accord with the unit-cell parameter $a = 27.2635(18)$ Å measured for the Fornovolasco sample, larger than that of synthetic $K_2Fe^{2+}{}_5Fe^{3+}{}_3Al(SO_4)_{12}(H_2O)_{18}$ (i.e., $a = 27.234$ Å [70]) and similar to that of the samples previously labeled as "monsmedite" (i.e., $a = 27.2587$ Å [69]). Biagioni et al. [15] discussed the crystal-chemistry of the studied sample, with a particular focus on the Tl speciation (studied through XAS) and reported FTIR and micro-Raman data.

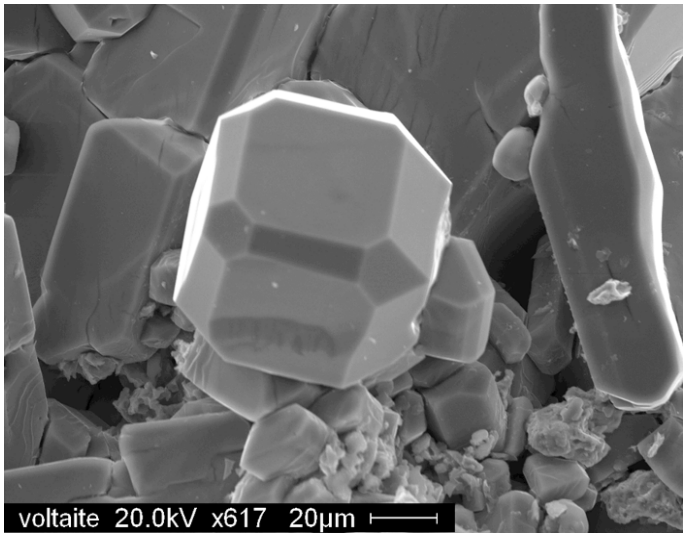

Figure 24. Voltaite from the Fornovolasco mine, as cubic crystals with minor {110} and {111} faces.

A new occurrence of voltaite has been recently identified in the sulfate assemblage from the Monte Arsiccio mine. Voltaite occurs as black compact veins or as euhedral crystals, with different habits: cubic {100}, octahedral {111}, and, rarely, rhombododecahedral {110} (Figure 25). In some cases, complex crystals showing the association of these three forms were observed. Euhedral crystals typically occur within fibrous halotrichite and directly grown on pyrite or, rarely, on schist, sometimes associated with melanterite, römerite, and krausite. These crystals can reach up to 2 cm on edge.

The identification of voltaite has been performed through SC-XRD, giving the unit-cell parameter a = 27.2214(7) Å. No chemical data are currently available for this recent finding.

Figure 25. Voltaite from the Monte Arsiccio mine, as up to 2 cm-sized octahedral crystals.

3.22. Wilcoxite

Wilcoxite is a rare fluo-sulfate, ideally $MgAl(SO_4)_2F(H_2O)_{11}\cdot 6H_2O$. Its occurrence in the secondary assemblages from the pyrite ores of the Apuan Alps was reported by Mauro et al. [28] on samples from the Fornovolasco mine, where wilcoxite occurs as colorless to whitish crystals, in some cases showing rounded edges, up to 5 mm across (Figure 26), associated with epsomite, gypsum, and an intermediate member of the halotrichite-pickeringite series [28]. Qualitative chemical analyses, performed in EDS mode, showed Mg, Al, S, F, and minor Fe as the only elements with $Z > 8$ above the detection limit. SC-XRD data pointed to a triclinic unit cell, with a = 6.6749(4), b = 6.7730(4), c = 14.9076(9) Å, α = 79.604(3), β = 80.163(3), γ = 62.475(3)°, space group P-1. Structural details, as well as micro-Raman spectroscopic features, are described in Mauro et al. [28].

Figure 26. Wilcoxite, triclinic colorless crystals, up to 5 mm in length, associated with colorless granular melanterite and acicular crystals of halotrichite-pickeringite from the Fornovolasco mine.

3.23. Other Sulfate-Bearing Phases

The secondary assemblages of the pyrite ores from the Apuan Alps are characterized by the occurrence of other sulfate-bearing phases, where the $(SO_4)^{2-}$ complex anion is associated with $(PO_4)^{3-}$ groups. Indeed, the presence of iron phosphates has been known since the study of Senesi [42], who reported the presence of koninckite, strengite, variscite, and, possibly, florencite-(Ce). Orlandi and Dini [71] reported the occurrence of diadochite from the Buca della Vena mine, whereas Biagioni [29] proposed to classify these samples as destinezite, owing to their crystalline nature (instead of, diadochite is amorphous [72]). Later, Mauro et al. [3], investigating some of these specimens, discovered the new mineral species bohuslavite. This mineral forms aggregates of tabular pseudohexagonal crystals, up to 0.25 mm in size, colorless to pinkish to lilac under artificial light and white to yellowish under natural light [3] (Figure 27a). It occurs in fractures of pyrite-bearing schist, along with gypsum and minor jarosite.

Figure 27. The two iron phosphate-sulfates occurring at the Buca della Vena mine. (**a**) Bohuslavite, as rounded aggregates of tabular pseudohexagonal crystals, up to 1 mm in size, with gypsum as colorless needles. (**b**) Destinezite, as microcrystalline pinkish masses, up to 3 mm in size.

Destinezite occurs at the Buca della Vena mine as microcrystalline whitish to pinkish aggregates (Figure 27b), in the same occurrence of bohuslavite. Its identification was performed through XRPD; similarly, destinezite was identified on the walls of old mining tunnels in the Pollone and Monte Arsiccio mines, as earthy efflorescences, white to lilac in color. These identifications were supported by XRPD data.

4. Field Observations

Sulfate mineral associations tend to evolve in space and time, reflecting the changes of physico-chemical conditions occurring during sulfide alteration [23]. Since the seminal work of Bandy [73], several authors have described the sequences of mineral phases observed in different localities worldwide. The general sequence, from early to late stage minerals, begins with melanterite (or some other $Fe^{2+}SO_4 \cdot nH_2O$ phase), evolving to mixed Fe^{2+}-Fe^{3+} and Fe^{3+}-only salts and then to jarosite and eventually to Fe oxy-hydroxides [23]. This sequence can be interpreted, in agreement with Jerz and Rimstidt [74], as due to a series of reactions of oxidation, neutralization, and dehydration. The knowledge of these associations is not a trivial exercise because they play a central role in controlling the fate of trace metals and acidity at AMD systems.

During this ten-years long study, two main localities have been studied with a special focus on sulfate parageneses, where the term paragenesis is used according to Jambor et al. [23]: the Fornovolasco and the Monte Arsiccio mines. Data on the other localities are still incomplete.

4.1. The Fornovolasco Mine

Mauro [51] described the occurrence of three sulfate piles in the old tunnels of the Fornovolasco mine (Figure 28), where pyrite ores are located close to the contact between schist and metadolostone. Primary ore is formed by pyrite with minor pyrrhotite, arsenopyrite, and stibnite and accessory sulfosalts (e.g., berthierite, jamesonite). Gangue minerals are siderite, quartz, chlorite, and stilpnomelane [7].

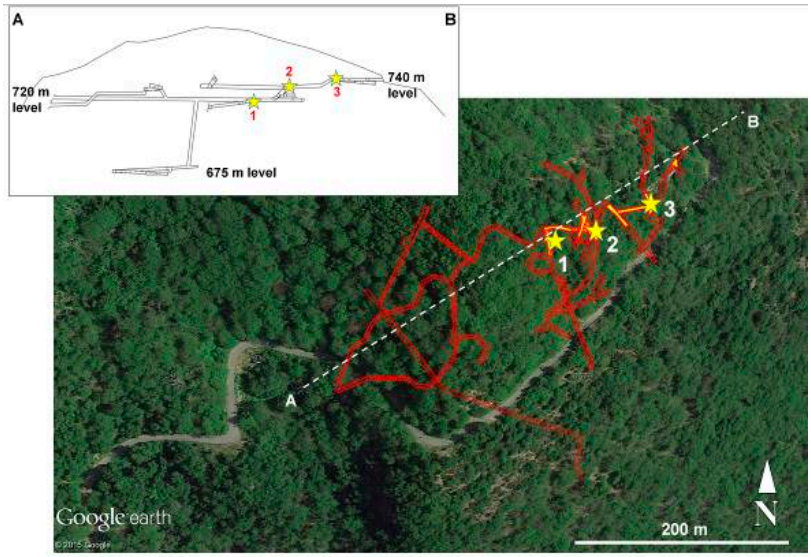

Figure 28. Planimetry of the Fornovolasco mine, showing the occurrence of the three sulfate piles in the old tunnels. Red lines represent the mining works, whereas pyrite ore bodies are shown as the yellow filling in the tunnels. Stars indicate the location of the sulfate piles. The A–B line gives the direction of the vertical section of the mining complex.

Sulfate pile #1 is in the level 720 m, and it measures $3.2 \times 2 \times 1$ m^3. Its mineralogy is very simple, being formed dominantly by microcrystalline pyrite, closely associated with melanterite, as fibrous greenish-bluish masses, and fibrous white halotrichite. No other phases have been observed. Pile #1 seems to represent an early stage of pyrite alteration.

Sulfate pile #2 is located in the 740 m level, at the top of an inclined shaft connecting this level with the underlying 720 m level. It measures $3.5 \times 3.1 \times 2.1$ m^3. Biagioni et al. [2] reported a mineralogical sequence observed within this pile, after the digging of a small trench (Figure 29). The core of the pile is formed by unaltered microcrystalline pyrite, intimately associated with melanterite. Toward the periphery, this core is followed by a mass of microcrystalline römerite. The transformation of melanterite into römerite (Figure 29) may be described through the oxidation–dehydration reaction $3FeSO_4 \cdot 7H_2O + H_2SO_4 + 0.5O_2 = Fe^{2+}Fe^{3+}{}_2(SO_4)_4 \cdot 14H_2O + 8H_2O$. Within this mass, there are vugs covered by euhedral individuals of römerite, needles of halotrichite, and microcrystalline aggregates of yellow-canary magnesiocopiapite. Rarely, greenish voltaite, gypsum, and octahedral alum-(K) were found. In addition, close to the contact with melanterite, this latter sulfate can occur in euhedral individuals within the small vugs of microcrystalline römerite. Halotrichite was found both with melanterite and römerite + magnesiocopiapite. On the outer zone of the sulfate pile, fibroferrite replaces melanterite, likely according to the oxidation-dehydration reaction $FeSO_4 \cdot 7H_2O + 0.25O_2 = Fe(SO_4)(OH) \cdot 5H_2O + 1.5H_2O$, in agreement with [74]. Volaschioite is strongly oxidized, being an oxy-hydroxy-hydrated Fe^{3+} sulfate, and it was found in a limited zone, in the outer portion of the sulfate pile. Close to the contact between the sulfate pile and metadolostone, epsomite was observed, along with gypsum. A jarosite subgroup mineral was found at the bottom of the sulfate pile and close to the contact with metadolostone, as microcrystalline aggregates associated with iron oxides ("limonite"). Secondary minerals occurring in this sulfate pile seem to be related to the progressive diffusion of

atmospheric O_2 within the pile, with Fe^{3+}-only sulfates in the outer portion, mixed Fe^{2+}-Fe^{3+} sulfates in the middle section, and melanterite at the core of the pile (Figure 29). The position of halotrichite is not well-constrained. As noted by Bandy [73], halotrichite is usually an early mineral, even if it occurs also as one of the efflorescent salts crystallizing after all the other species, suggesting that this mineral (as well as its Mg isotype pickeringite) may be stable in a wide range of conditions.

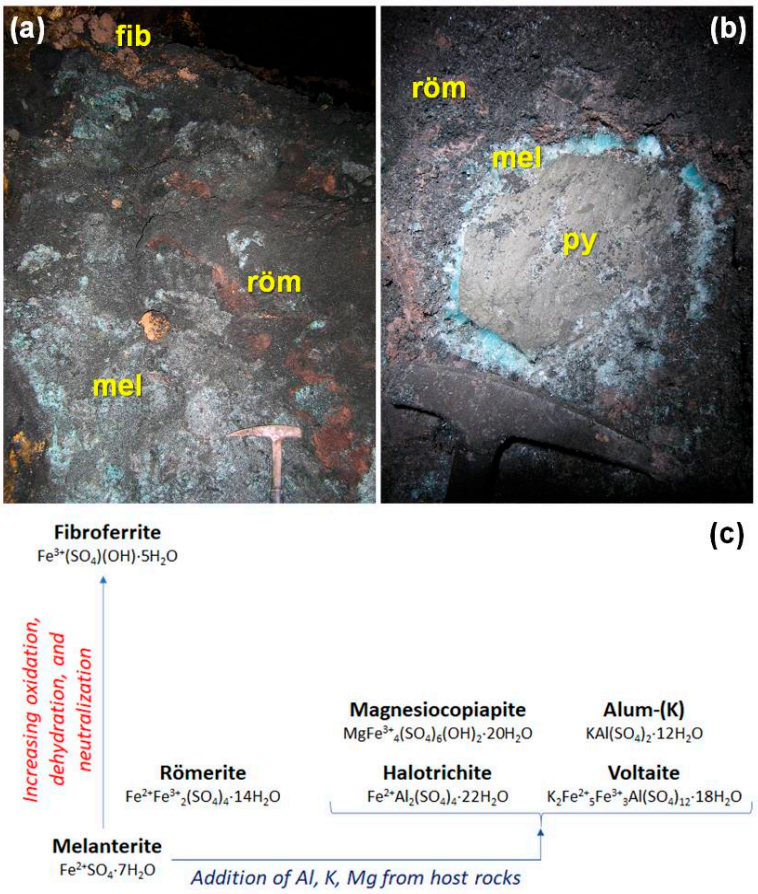

Figure 29. (**a**) Vertical section in the sulfate pile #2 in the Fornovolasco mine, showing, from the core to the rim, the sequence melanterite (mel)—römerite (röm)—fibroferrite (fib); in (**b**), the sequence melanterite-römerite can be observed around unaltered fragments of pyrite (py). An interpretation of the observed sulfate association, limited to the main phases, is given in (**c**).

Potassium salts, i.e., alum-(K) and voltaite, are not common, and their relative rarity may be due to the rarity of K-bearing phases in the primary pyrite ores and in the country rock. A peculiar feature of some secondary K-bearing sulfates identified in pile #2 is the presence of (NH_4) and Tl replacing K. Whereas the latter was not unexpected, owing to the high Tl contents of pyrite ores from Fornovolasco [7–9], the former was not predictable. Its occurrence seems to be related to the presence of carbonaceous matter in pyrite ores. Other phases reported at the Fornovolasco mine (alunogen, coquimbite, krausite, rhomboclase, and a fraction of the observed voltaite) are likely tertiary minerals, following the definition given by Jambor [75], that is they are formed after human disturbance (i.e., during drying after the sample removal from the original occurrence).

Sulfate pile #3 is located on the 740 m level, in an area where acidic solutions deriving from pyrite oxidation interacts with metadolostone. In this occurrence, along with melanterite, magnesiocopiapite, and an intermediate member of the halotrichite-pickeringite series, epsomite and gypsum are rather common, likely deriving from the interaction between metadolostone and H_2SO_4, according to the reaction $CaMg(CO_3)_2 + 2H_2SO_4 + 7H_2O = Mg(SO_4)\cdot 7H_2O + Ca(SO_4)\cdot 2H_2O + 2CO_2$. An interesting feature of this pile is the occurrence of the fluo-sulfate wilcoxite. The source of F is not known; however,

it could be hypothesized that a role may be played by phyllosilicates, also able to provide Al, occurring in halotrichite-pickeringite and wilcoxite.

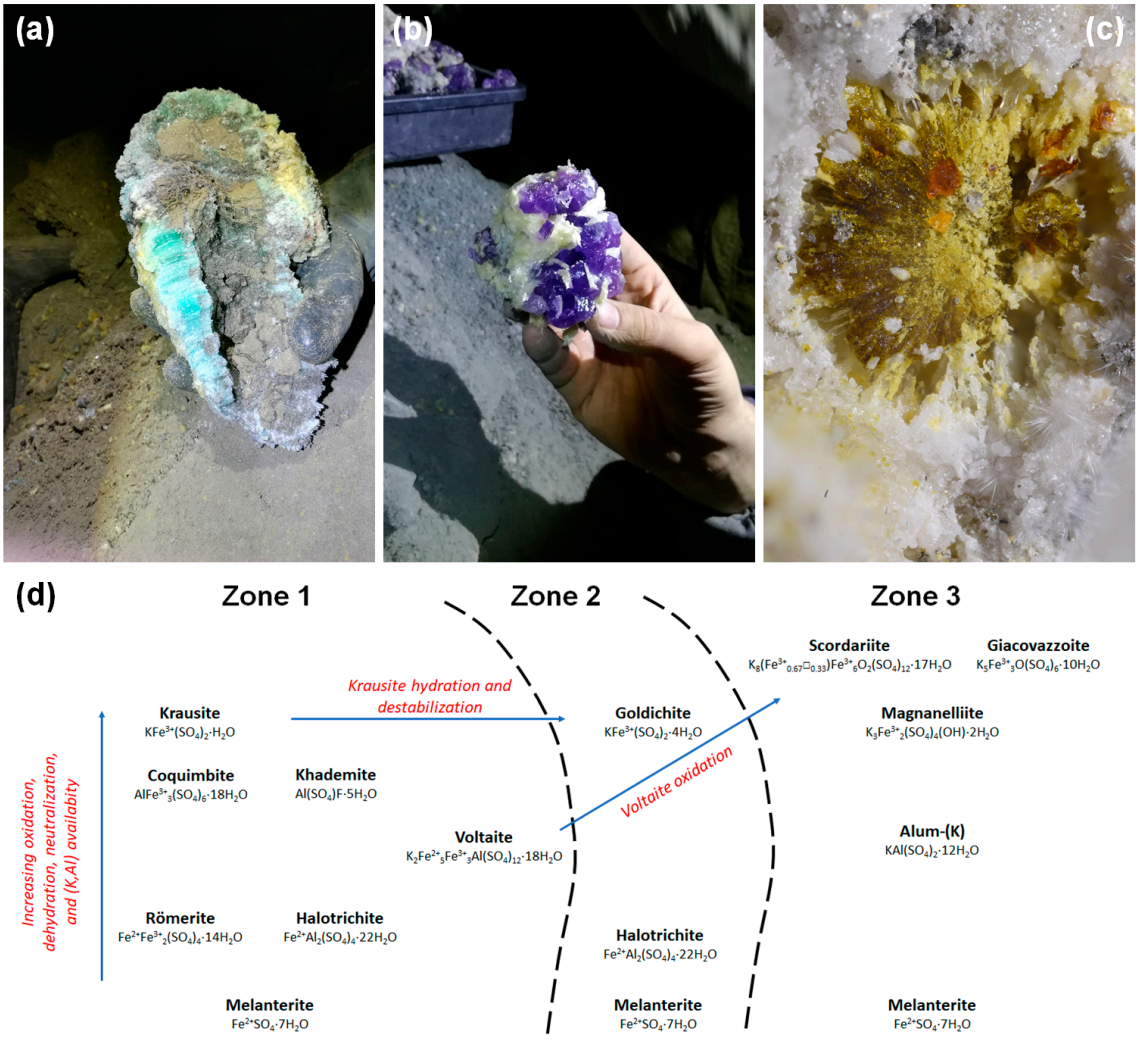

Figure 30. Melanterite is the first oxidation product of pyrite in the Monte Arsiccio mine (**a**). In the sulfate sequence, it is followed by several species, showing increasing oxidation and the addition of other elements (e.g., K, Al). Several of these species (voltaite, coquimbite, krausite) are included in halotrichite, as exemplified by the purple crystals of coquimbite embedded in fibrous white halotrichite (**b**). Krausite, in the outer portion of the sulfate assemblage, tends to hydrate and to be destabilized, being replaced by other phases. In (**c**), a radial aggregate of krausite, 5 mm in diameter, is almost fully replaced by magnanelliite, scordariite, and giacovazzoite, and it is embedded in alum-(K). In (**d**), the most characteristic species identified in the Monte Arsiccio sulfate assemblage are reported, according to their occurrence in different zones, from the core of the pyrite ore body (Zone 1) towards the surface (Zone 3), passing through the intermediate Zone 2.

4.2. The Monte Arsiccio Mine

The Monte Arsiccio mine has some geological features required to maximize the pyrite oxidation and the acid generation: (i) ore with a high pyrite content, (ii) low capacity of acid neutralization by the phylladic rocks, (iii) easy availability of atmospheric O_2 and H_2O in porous and undersaturated conditions, due both to the geological nature of the area, with the phylladic mineralized rocks underlying strongly fractured and karstified metadolostone, and to the mining workings, favouring the infiltration of both air and water in the underground. In addition, the presence of microbiological

activity [9] is able to enhance the pyrite oxidation. These features are like those described for the well-known AMD site of Iron Mountain, California [76].

In addition to minor sulfate occurrences (e.g., epsomite formed on metadolostone) and to the widespread presence of gypsum on the walls of mining works, the main attention is focused on the most important sulfate assemblage where more than 15 different mineral species have been identified, among which the three new K-Fe^{3+} sulfates giacovazzoite, magnanelliite, and scordariite [4–6]. Here, a microcrystalline pyrite ore body is embedded within whitish quartzitic phyllites, mineralogically formed by quartz and mica with variable amounts of chlorite, with tourmalinite layers representing a common feature. As reported by Vezzoni et al. [77], these rocks are enriched in K_2O, likely as a consequence of a Permian hydrothermal alteration event. This K_2O enrichment is likely the main reason for the abundance of K-sulfates in the assemblage from Monte Arsiccio, where the action of H_2SO_4 is able to cause the leaching of aluminosilicates, that may be the main source of K [23].

Pyrite ore body and host rocks are cut by veins filled by sulfate minerals. The first oxidation product is melanterite, occurring as light blue fibers closely associated with pyrite (Figure 30). As regards the iron sulfates, the typical sequence starting from melanterite and giving rise to Fe^{2+}-Fe^{3+} and eventually Fe^{3+}-only sulfates is observed. In particular, the crystallization of melanterite is followed by that of römerite. The latter tends to alter to coquimbite, with the full Fe oxidation and the introduction of Al into the system, likely due to the leaching of country rocks. The replacement of römerite by coquimbite was reported by previous authors (e.g., [19]). Aluminum is also an essential chemical constituent of halotrichite, whose position in the sulfate assemblage is not clear. Indeed, it was observed in vugs of römerite veins, or as veins in the pyrite ore hosting, sometimes, coquimbite (Figure 30) or voltaite. As written above, and in agreement with previous authors (e.g., [73]), halotrichite seems to be stable in a wide range of conditions. Late-stage fluids seem to favour the crystallization of krausite and minor khademite. The latter is a fluo-sulfate. Recently, Lacalamita et al. [78] detected high F content in micas from the Monte Arsiccio mine; these phases may be the source not only of K and Al, but also for F. Krausite was observed as overgrowths on the other sulfates (i.e., römerite, coquimbite—Figure 17) and it has been found also on alunogen and halotrichite. Krausite seems to postdate the crystallization of alunogen, whose individuals are superficially corroded, whereas krausite crystals are shiny, without any hints of alteration. This association was observed within the ore body (Zone 1 in Figure 30), whereas on the surface, exposed to air moisture, some differences can be reported.

Towards the surface of the exposed ore body, krausite is replaced by goldichite, having a higher hydration state and usually occurring within halotrichite (Zone 2 in Figure 30). Finally, in the outer portion of the ore body (Zone 3 in Figure 30), melanterite and alum-(K) seems to be the most common phases. It is worth noting that the position of the outer surface likely changes in time, since the crystallization of sulfates favours the brecciation of the ore body and country rocks, promoting their collapse in the exploitation void. For this reason, the occurrence of melanterite is likely related to the rapid oxidation of recently exposed and unaltered pyrite, whereas alum-(K) can be the result of the interaction of H_2SO_4 with country rocks and of the replacement of krausite. The retreat of the exposed surface, owing to its collapse promoted by sulfate crystallization, may favor the exposure of the sulfate assemblages formed within the ore body (Zone 1). This assemblage may not be in equilibrium with the different conditions occurring in the external portion of the ore body (for instance, römerite could be easily dissolved by the higher relative humidity) and some changes can occur. Among them, the study of the available specimens suggests that krausite may be no longer stable. Since this mineral is a K-Fe^{3+} sulfate, minor Fe^{3+} observed in alum-(K) could be an inheritance of the former phase. In addition, some textural features suggest that krausite is replaced by magnanelliite and could be also related to the crystallization of giacovazzoite and scordariite (Figure 30). As suggested by [4], giacovazzoite may derive also from the breakdown of Fe-rich domains of alum-(K). Whereas the active role of krausite in promoting the crystallization of these new mineral species is suggested by textural observations, the importance of voltaite in this respect has not been fully understood yet. However, the finding of a specimen showing a cubic crystal of voltaite deeply corroded and superficially altered in alum-(K),

goldichite, and, finally, scordariite, supports the hypothesis that also the late-stage alteration of voltaite may play a role in determining the complex mineralogy of the K-Fe sulfate assemblage observed at the Monte Arsiccio mine. All the new mineral phases have been observed only on the surface of the exposed ore body (Zone 3).

Finally, jarosite was observed in association with magnanelliite and it may indicate the precipitation from low-*p*H sulfate-rich pore waters, during the final stages of the evolution of the sulfate assemblage from the Monte Arsiccio mine.

5. Conclusions

Hydrothermal ore deposits from the Apuan Alps have been known since the middle of the 19th century for the occurrence of well-crystallized mineral specimens, mainly represented by sulfides and sulfosalts. During the second half of the 20th century and the first decades of the 21st century, the mineralogical study of these deposits revealed an unexpected complexity, mirroring the geochemical features that have been detected only very recently (e.g., [7–9]). Secondary minerals were almost totally neglected by previous mineralogical investigations. Only since the middle of the 2000s, the studies performed in the Fornovolasco mine have begun to reveal the occurrence of interesting associations, representing a valuable link between mineral systematics and environmental mineralogy. The further discovery of other assemblages and, in particular, that occurring in the Monte Arsiccio mine, promoted additional studies, favoured by the well-crystallized nature of several phases. New crystal-chemical data were collected and some new mineral species were discovered, indicating that the pyrite ores of the Apuan Alps can be considered as a reference locality for the study of alteration processes of this iron sulfide and the evolution of secondary minerals, resulting from the interplay between lithosphere, atmosphere, hydrosphere, and biosphere.

Author Contributions: C.B. and D.M. wrote the manuscript, with input from M.P. All authors have read and agreed to the published version of the manuscript.

Funding: This research received support by the University of Pisa through the project P.R.A. 2018–2019 "Georisorse e Ambiente" (Grant No. PRA_2018_41).

Acknowledgments: The following mineral collectors, who provided mineral specimens used in this ten-years long study, are warmly acknowledged (in alphabetical order): Tiberio Bardi, Mario Bianchini, Giorgio Pezzini, Luigi Pierotti, Giovanni Polacci, Ugo Quilici, Moreno Romani, and Carlo Zanelli. In addition, we would like to thank the colleagues who helped us in this study (in alphabetical order): Luca Bindi, Elena Bonaccorsi, Ulf Hålenius, Anthony R. Kampf, Giovanni Orazio Lepore, Paolo Orlandi, Henrik Skogby, and Federica Zaccarini. We would like to thank our colleague Massimo D'Orazio for his critical reading of a first draft of this manuscript. The paper was improved by the comments of two anonymous reviewers.

Conflicts of Interest: The authors declare no conflict of interest.

References

1. D'Achiardi, A. *Mineralogia della Toscana*; Tipografia Nistri: Pisa, Italy, 1872; Volume 1, p. 276.
2. Biagioni, C.; Bonaccorsi, E.; Orlandi, P. Volaschioite, $Fe^{3+}_4(SO_4)O_2(OH)_6{\cdot}2H_2O$, a new mineral species from Fornovolasco, Apuan Alps, Tuscany, Italy. *Can. Miner.* **2011**, *49*, 605–614. [CrossRef]
3. Mauro, D.; Biagioni, C.; Bonaccorsi, E.; Hålenius, U.; Pasero, M.; Skogby, H.; Zaccarini, F.; Sejkora, J.; Plášil, J.; Kampf, A.R.; et al. Bohuslavite, $Fe^{3+}_4(PO_4)_3(SO_4)(OH)(H_2O)_{10}{\cdot}nH_2O$, a new hydrated iron phosphate-sulfate. *Eur. J. Miner.* **2019**, *31*, 1033–1046. [CrossRef]
4. Biagioni, C.; Bindi, L.; Mauro, D.; Pasero, M. Crystal-chemistry of sulfates from the Apuan Alps (Tuscany, Italy). IV. Giacovazzoite, $K_5Fe^{3+}_3O(SO_4)_6(H_2O)_9{\cdot}H_2O$, the natural analogue of the β-Maus's Salt and its dehydration product. *Phys. Chem. Miner.* **2020**, *47*, 7. [CrossRef]
5. Biagioni, C.; Bindi, L.; Mauro, D.; Hålenius, U. Crystal chemistry of sulfates from the Apuan Alps (Tuscany, Italy). V. Scordariite, $K_8(Fe^{3+}_{0.67}\square_{0.33})[Fe^{3+}_3O(SO_4)_6(H_2O)_3]_2(H_2O)_{11}$: A new metavoltine-related mineral. *Minerals* **2019**, *9*, 702. [CrossRef]

6. Biagioni, C.; Bindi, L.; Kampf, A.R. Crystal chemistry of sulfates from the Apuan Alps (Tuscany, Italy). VII. Magnanelliite, $K_3Fe^{3+}{}_2(SO_4)_4(OH)(H_2O)_2$, a new sulfate from the Monte Arsiccio mine. *Minerals* **2019**, *9*, 779. [CrossRef]
7. George, L.L.; Biagioni, C.; D'Orazio, M.; Cook, N.J. Textural and trace element evolution of pyrite during greenschist facies metamorphic recrystallization in the southern Apuan Alps (Tuscany, Italy): Influence on the formation of Tl-rich sulfosalt melt. *Ore Geol. Rev.* **2018**, *102*, 59–105. [CrossRef]
8. Biagioni, C.; D'Orazio, M.; Vezzoni, S.; Dini, A.; Orlandi, P. Mobilization of Tl-Hg-As-Sb-(Ag,Cu)-Pb sulfosalt melts during low-grade metamorphism in the Alpi Apuane (Tuscany, Italy). *Geology* **2013**, *41*, 747–750. [CrossRef]
9. D'Orazio, M.; Biagioni, C.; Dini, A.; Vezzoni, S. Thallium-rich pyrite ores from the Apuan Alps, Tuscany, Italy: Constraints for their origin and environmental concerns. *Miner. Depos.* **2017**, *52*, 687–707. [CrossRef]
10. Lattanzi, P.; Benvenuti, M.; Costagliola, P.; Tanelli, G. An overview on recent research on the metallogeny of Tuscany, with special reference to the Apuan Alps. *Mem. Soc. Geol. Ital.* **1994**, *48*, 613–625.
11. Giannecchini, R. Relationship between rainfall and shallow landslides in the southern Apuan Alps (Italy). *Nat. Hazards Earth Syst. Sci.* **2006**, *186*, 357–364. [CrossRef]
12. Perotti, M.; Petrini, R.; D'Orazio, M.; Ghezzi, L.; Giannecchini, R.; Vezzoni, S. Thallium and other potentially toxic elements in the Baccatoio stream catchment (northern Tuscany, Italy) receiving drainages from abandoned mines. *Mine Water Environ.* **2018**, *37*, 431–441. [CrossRef]
13. Ciriotti, M.E.; Fascio, L.; Pasero, M. *Italian Type Minerals*; Edizioni PLUS: Pisa, Italy, 2009; p. 360.
14. Palache, C.; Berman, H.; Frondel, C. *System of Mineralogy*, 7th ed.; John, Wiley and Sons: New York, NY, USA, 1952.
15. Biagioni, C.; Mauro, D.; Pasero, M.; Bonaccorsi, E.; Lepore, G.O.; Zaccarini, F.; Skogby, H. Crystal chemistry of sulfates from the Apuan Alps (Tuscany, Italy). VI. Thallium-bearing alum-(K) and voltaite from the Fornovolasco mining complex. *Am. Miner.* **2020**, *105*, 1088–1098. [CrossRef]
16. Ballirano, P. Thermal behaviour of alum-(K) $KAl(SO_4)_2{\cdot}12H_2O$ from *in situ* laboratory high-temperature powder X-ray diffraction data: Thermal expansion and modelling of the sulfate orientational disorder. *Miner. Mag.* **2015**, *79*, 157–170. [CrossRef]
17. Nyburg, S.C.; Steed, J.W.; Aleksovska, S.; Petrusevski, V.M. Structure of the alums. I. On the sulfate group disorder in the α-alums. *Acta Cryst.* **2000**, *B56*, 204–209. [CrossRef] [PubMed]
18. Mauro, D. Crystal-Chemistry of the Secondary Minerals of Thallium-Rich Pyrite Ores from the Apuan Alps (Tuscany, Italy). Ph.D. Thesis, University of Pisa, Pisa, Italy, 2020.
19. Bariand, P.; Cesbron, F.; Berthelon, J.-P. Les sulfates de fer de Saghand près de Yazd (Iran). *Mem. Hors-Série Soc. Geol. Fr.* **1977**, *8*, 77–85.
20. Menchetti, S.; Sabelli, C. Alunogen: Its structure and twinning. *Tschermaks Min. Petr. Mitt.* **1974**, *21*, 164–178. [CrossRef]
21. Fang, J.H.; Robinson, P.D. Alunogen, $Al_2(H_2O)_{12}(SO_4)_3{\cdot}5H_2O$: Its atomic arrangement and water content. *Am. Miner.* **1976**, *61*, 311–317.
22. Foshag, W.F. Krausite, a new sulfate from California. *Am. Miner.* **1931**, *16*, 352–360.
23. Jambor, J.L.; Nordstrom, K.D.; Alpers, C.N. Metal-sulfates salts from sulfide minerals oxidation. In. Sulfate minerals—Crystallography, geochemistry and environmental significance. *Rev. Miner. Geochem.* **2000**, *40*, 305–340. [CrossRef]
24. Fanfani, L.; Nunzi, A.; Zanazzi, P.F.; Zanzari, A.R. The copiapite problem: The crystal structure of a ferrian copiapite. *Am. Miner.* **1973**, *58*, 314–322.
25. Majzlan, J.; Kiefer, B. An X-ray and neutron-diffraction study of synthetic ferricopiapite, $Fe_{14/3}(SO_4)_6(OD,OH)_2(D_2O,H_2O)_{20}$, and *ab initio* calculations on the structure of magnesiocopiapite, $MgFe_4(SO_4)_6(OH)_2(H_2O)_{20}$. *Can. Miner.* **2006**, *44*, 1227–1237. [CrossRef]
26. Majzlan, J.; Michallik, R. The crystal structures, solid solutions and infrared spectra of copiapite-group minerals. *Miner. Mag.* **2007**, *71*, 553–569. [CrossRef]
27. Biagioni, C.; Orlandi, P.; Bonini, M. Fornovolasco. Storia e minerali delle miniere di ferro presso Vergemoli (Alpi Apuane). *Riv. Miner. Ital.* **2008**, *32*, 230–252.
28. Mauro, D.; Biagioni, C.; Pasero, M.; Skogby, H. Crystal-chemistry of sulfates from the Apuan Alps (Tuscany, Italy). III. Mg-rich sulfate assemblages from the Fornovolasco mining complex. *Atti Soc. Tosc. Sci. Nat. Mem.* **2019**, *126*, 33–44.

29. Biagioni, C. *Minerali della Provincia di Lucca*; Associazione Micro-Mineralogica Italiana: Cremona, Italy, 2009; 352p.
30. Mauro, D.; Biagioni, C.; Pasero, M.; Skogby, H.; Zaccarini, F. Redefinition of coquimbite, $AlFe^{3+}{}_3(SO_4)_6(H_2O)_{12}{\cdot}6H_2O$. *Miner. Mag.* **2020**, *84*, 275–282. [CrossRef]
31. Ventruti, G.; Della Ventura, G.; Bellatreccia, F.; Lacalamita, M.; Schingaro, E. Hydrogen bond system and vibrational spectroscopy of the iron sulfate fibroferrite, $Fe(OH)SO_4{\cdot}5H_2O$. *Eur. J. Miner.* **2016**, *28*, 943–952. [CrossRef]
32. Scordari, F.; Stasi, F.; Schingaro, E.; Comunale, G. A survey of $(Na,H_3O^+,K)_5Fe_3O(SO_4)_6{\cdot}H_2O$ compounds: Architectural principles and influence of the Na-K replacement on their structures. Crystal structure, solid-state transformation and its relationship to some analogues. *Z. Krist.* **1994**, *209*, 733–736.
33. Mereiter, V.K.; Völlenkle, H. Die Kristallstruktur von β-pentakalium-[μ_3-oxo-hexa-μ-sulfato-triaquatrieisen (III)]-Heptahydrat-eine monocline Modifikation des Mausschen Salzes. *Acta Cryst.* **1978**, *B34*, 378–384. [CrossRef]
34. Rosenzweig, A.; Gross, E.B. Goldichite, a new hydrous potassium ferric sulfate from the San Rafael Swell, Utah. *Am. Miner.* **1955**, *40*, 469–480.
35. Márquez-Zavalía, M.F.; Galliski, M.A. Goldichite of fumarolic origin from the Santa Bárbara mine, Jujuy, nortwestern Argentina. *Can. Miner.* **1995**, *33*, 1059–1062.
36. Russo, M.; Campostrini, I.; Demartin, F. I minerali di origine fumarolica dei Campi Flegrei: Solfatara di Pozzuoli (Napoli) e dintorni. *MICRO* **2017**, *15*, 122–192.
37. Graeber, E.J.; Rosenzweig, A. The crystal structure of yavapaiite, $KFe(SO_4)_2$, and goldichite, $KFe(SO_4)_2{\cdot}4H_2O$. *Am. Miner.* **1971**, *56*, 1917–1933.
38. Yang, Z.; Giester, G. Hydrogen bonding in goldichite, $KFe(SO_4)_2{\cdot}4H_2O$: Structure refinement. *Miner. Petrol.* **2018**, *112*, 135–142. [CrossRef]
39. Bayliss, P.; Kolitsch, U.; Nickel, E.H.; Pring, A. Alunite supergroup: Recommended nomenclature. *Miner. Mag.* **2010**, *74*, 919–927. [CrossRef]
40. Dutrizac, J.E.; Jambor, J.L. Jarosites and their application in hydrometallurgy. In: Sulfate minerals—Crystallography, geochemistry and environmental significance. *Rev. Miner. Geochem.* **2000**, *40*, 405–452. [CrossRef]
41. Stoffregen, R.E.; Alpers, C.N.; Jambor, J.L. Alunite-jarosite crystallography, thermodynamics, and geochronology. In. Sulfate minerals—Crystallography, geochemistry and environmental significance. *Rev. Miner. Geochem.* **2000**, *40*, 453–479. [CrossRef]
42. Senesi, F. Koninckite e altri fosfati della miniera del Pollone (Valdicastello Carducci, Lucca). *Riv. Miner. Ital.* **2000**, *24*, 46–48.
43. Holland, T.J.B.; Redfern, S.A.T. Unit cell refinement from powder diffraction data: The use of regression diagnostics. *Miner. Mag.* **1997**, *61*, 65–77. [CrossRef]
44. Sasaki, K.; Tanaike, O.; Konno, H. Distinction of jarosite-group compounds by Raman spectroscopy. *Can. Miner.* **1998**, *36*, 1225–1235.
45. Basciano, L.C.; Peterson, R.C. The crystal structure of ammoniojarosite, $(NH_4)Fe_3(SO_4)_2(OH)_6$ and the crystal chemistry of ammoniojarosite–hydronium jarosite solid-solution series. *Miner. Mag.* **2007**, *71*, 427–441. [CrossRef]
46. Basciano, L.C.; Peterson, R.C. Jarosite-hydronium jarosite solid-solution series with full iron occupancy: Mineralogy and crystal chemistry. *Am. Miner.* **2007**, *92*, 1464–1473. [CrossRef]
47. Plášil, J.; Škoda, R.; Fejfarová, K.; Čejka, J.; Kasatkin, A.V.; Dušek, M.; Talla, D.; Lapčák, L.; Machovič, V.; Dini, M. Hydroniumjarosite, $(H_3O)^+Fe_3(SO_4)_2(OH)_6$, from Cerros Pintados, Chile: Single-crystal X-ray diffraction and vibrational spectroscopic study. *Miner. Mag.* **2014**, *78*, 535–547. [CrossRef]
48. Chio, C.H.; Sharma, S.K.; Ming, L.-C.; Muenow, D.W. Raman spectroscopic investigation on jarosite-yavapaiite stability. *Spectrochim. Acta Part A Mol. Biomol. Spectrosc.* **2010**, *75*, 162–171. [CrossRef] [PubMed]
49. Košek, F.; Žáček, V.; Škoda, R.; Laufek, F.; Jehlička, J. New mineralogical data for khademite (orthorhombic $AlSO_4F{\cdot}5H_2O$) and the story of rostite (orthorhombic $AlSO_4OH{\cdot}5H_2O$) from Libušín, near Kladno, Czech Republic. *J. Mol. Struct.* **2019**, *1175*, 208–213. [CrossRef]
50. Mauro, D.; Biagioni, C.; Pasero, M.; Zaccarini, F. Crystal-chemistry of sulfates from the Apuan Alps, Tuscany, Italy. VIII. New data on khademite, $Al(SO_4)F(H_2O)_5$. *Miner. Mag.* **2020**, *84*, 540–546. [CrossRef]

51. Mauro, D. Studio cristallochimico di alcuni solfati di ferro della mineralizzazione a pirite tallifera di Fornovolasco (Alpi Apuane). Unpublished. Master's Thesis, University of Pisa, Pisa, Italy, 2016.
52. Graeber, E.J.; Morosin, B.; Rosenzweig, A. The crystal structure of krausite, $KFe(SO_4)_2 \cdot H_2O$. *Am. Miner.* **1965**, *50*, 1929–1936.
53. Effenberger, H.; Pertlik, F.; Zemann, J. Refinement of the crystal structure of krausite: A mineral with an interpolyhedral oxygen-oxygen contact shorter than the hydrogen bond. *Am. Miner.* **1986**, *71*, 202–205.
54. Kampf, A.R.; Mills, S.J.; Housley, R.M.; Williams, P.A.; Dini, M.A. Alcaparrosaite, $K_3Ti^{4+}Fe^{3+}(SO_4)_4O(H_2O)_2$, a new hydrophobic Ti^{4+} sulfate from Alcaparrosa, Chile. *Miner. Mag.* **2012**, *76*, 851–861. [CrossRef]
55. Targioni Tozzetti, G. *Relazioni D'alcuni Viaggi Fatti in Diverse Parti Della Toscana per Osservare le Produzioni Naturali, e gli Antichi Monumenti di Essa*, 2nd ed.; Stamperia Granducale: Firenze, Italy, 1773; p. 430.
56. Mauro, D.; Biagioni, C.; Pasero, M. Crystal-chemistry of sulfates from Apuan Alps (Tuscany, Italy). I. Crystal structure and hydrogen bond system of melanterite, $Fe(H_2O)_6(SO_4) \cdot H_2O$. *Period. Miner.* **2018**, *87*, 89–96.
57. Mauro, D.; Biagioni, C.; Pasero, M.; Zaccarini, F. Crystal-chemistry of sulfates from Apuan Alps (Tuscany, Italy). II. Crystal structure and hydrogen bonding system of römerite, $Fe^{2+}Fe^{3+}{}_2(SO_4)_4(H_2O)_{14}$. *Atti Soc. Tosc. Sci. Nat. Mem.* **2018**, *125*, 5–11.
58. Oleinikov, B.V.; Shvartsev, S.L. Contemporary sulfate formation in the zone of oxidation of pyrrhotite-chalcopyrite hydrothermal ores, northwestern Siberian Platform. *Geol. Geofiz.* **1968**, *6*, 15–25.
59. Giacovazzo, C.; Scordari, F.; Todisco, A.; Menchetti, S. Crystal structure model for metavoltine from Sierra Gorda. *Tschermaks Miner. Petrogr. Mitt.* **1976**, *23*, 155–166. [CrossRef]
60. Giacovazzo, C.; Scordari, F.; Menchetti, S. Hydrous potassium and ferric iron sulphate (Maus's Salt). *Acta Cryst.* **1975**, *B31*, 2171–2173. [CrossRef]
61. Mills, S.J.; Kampf, A.R.; McDonald, A.M.; Bindi, L.; Christy, A.G.; Kolitsch, U.; Favreau, G. The crystal structure of parnauite: A copper arsenate-sulfate with translational disorder of structural rods. *Eur. J. Miner.* **2013**, *25*, 693–704. [CrossRef]
62. Walter Lévy, L.; Quéméneur, E. Étude de l'hydrolise du sulfate ferrique de 25 à 200°. *Bull. Soc. Chim. Fr.* **1966**, *6*, 1947–1954.
63. Fojt, B. On the problem of glockerite as a secondary mineral of ore deposits. *Scr. Fac. Sci. Nat. Ujep Brun. Geol. I* **1975**, *5*, 5–20.
64. Bigham, J.M.; Nordstrom, D.K. Iron and aluminum hydroxysulfates from acid sulfate waters. In: Sulfate Minerals—Crystallography, Geochemistry, and Environmental Significance (C.N. Alpers, J.L. Jambor and D.K Nordstrom ed.). *Rev. Miner. Geochem.* **2000**, *40*, 351–403. [CrossRef]
65. Manilici, V.; Giusca, D.; Stiopol, V. Studiul zacamintului de la Baia Sprie (Reg. Baia Mare). *Mem. Com. Geol.* **1965**, *7*, 1–113.
66. Götz, A.; Mihalka, S.; Ionita, I.; Toth, Z. Monsmeditul—Un nuo mineral de taliu de la Baia Sprie. *Rev. Miner.* **1968**, *19*, 154–159.
67. Zemann, J. What is monsmedite? *Rom. J. Miner.* **1993**, *76*, 97–98.
68. Johan, Z.; Udubasa, G.; Zemann, J. "Monsmedite", a discredited potassium thallium sulphate mineral from Baia Sprie and its identity with voltaite: The state of the art. *N. Jahr. Miner. Abh.* **2009**, *186*, 63–66. [CrossRef]
69. Kovács-Pálffy, P.; Muske, J.; Földvári, M.; Kónya, P.; Homonnay, Z.; Ntaflos, T.; Papp, G.; Király, E.; Sajó, I.; Szilágyi, V.; et al. Detailed study of "monsmedite" specimens from the original (1963) find, Baia Sprie, Baia Mare Ore District (Romania). *Carpath. J. Earth Environ. Sci.* **2011**, *6*, 321–330.
70. Mereiter, K. Die Kristallstruktur des Voltaits, $K_2Fe^{2+}{}_5Fe^{3+}{}_3Al[SO_4]_{12} \cdot 18H_2O$. *Tschermaks Miner. Petrogr. Mitt.* **1972**, *18*, 185–202. [CrossRef]
71. Orlandi, P.; Dini, A. Die Mineralien der Buca della Vena-Mine, Apuaner Berge, Toskana (Italien). *Lapis* **2004**, *29*, 11–24.
72. Peacor, D.R.; Rouse, R.C.; Coskren, T.D.; Essene, E.J. Destinezite ("diadochite"), $Fe_2(PO_4)(SO_4)(OH) \cdot 6H_2O$: Its crystal structure and role as a soil mineral at Alum Cave Bluff, Tennessee. *Clays Clay Miner.* **1999**, *47*, 1–11. [CrossRef]
73. Bandy, M.C. Mineralogy of three sulphate deposits of Northern Chile. *Am. Miner* **1938**, *23*, 669–760.
74. Jerz, J.K.; Rimstidt, J.D. Efflorescent iron sulfate minerals: Paragenesis, relative stability, and environmental impact. *Am. Miner.* **2003**, *88*, 1919–1932. [CrossRef]
75. Jambor, J.L. Mineralogy of sulfide-rich tailings and their oxidation products. *Environ. Geochem. Sulfide Mine-Wastes* **1994**, *22*, 59–102.

76. Jamieson, H.E.; Robinson, C.; Alpers, C.N.; McCleskey, R.B.; Nordstrom, D.K.; Peterson, R.C. Major and trace element composition of copiapite-group minerals and coexisting water from the Richmond mine, Iron Mountain, California. *Chem. Geol.* **2005**, *215*, 387–405. [CrossRef]
77. Vezzoni, S.; Pieruccioni, D.; Galanti, Y.; Biagioni, C.; Dini, A. Permian hydrothermal alteration preserved in polymetamorphic basement and constraints for ore-genesis (Alpi Apuane, Italy). *Geosciences* **2020**, *10*, 399. [CrossRef]
78. Lacalamita, M.; Schingaro, E.; Mesto, E.; Zaccarini, F.; Biagioni, C. Crystal-chemistry of micas belonging to the yangzhumingite-fluorophlogopite and phlogopite-fluorophlogopite series from the Apuan Alps (northern Tuscany, Italy). *Phys. Chem. Miner.* **2020**, *47*, 54. [CrossRef]